

Asymptotic correction approach to improving approximate exchange–correlation potentials: Time-dependent density-functional theory calculations of molecular excitation spectra

Mark E. Casida^{a)} and Dennis R. Salahub

Département de Chimie, Université de Montréal, Case Postale 6128, Succursale Centre-ville, Montréal, Québec H3C 3J7, Canada

(Received 7 May 1999; accepted 1 September 2000)

The time-dependent density functional theory (TD-DFT) calculation of excitation spectra places certain demands on the DFT exchange–correlation potential, v_{xc} , that are not met by the functionals normally used in molecular calculations. In particular, for high-lying excitations, it is crucial that the asymptotic behavior of v_{xc} be correct. In a previous paper, we introduced a novel asymptotic-correction approach which we used with the local density approximation (LDA) to yield an asymptotically corrected LDA (AC-LDA) potential [Casida, Casida, and Salahub, *Int. J. Quantum Chem.* **70**, 933 (1998)]. The present paper details the theory underlying this asymptotic correction approach, which involves a constant shift to incorporate the effect of the derivative discontinuity (DD) in the bulk region of finite systems, and a spliced asymptotic correction in the large r region. This is done without introducing any adjustable parameters. We emphasize that correcting the asymptotic behavior of v_{xc} is not by itself sufficient to improve the overall form of the potential unless the effect of the derivative discontinuity is taken into account. The approach could be used to correct v_{xc} from any of the commonly used gradient-corrected functionals. It is here applied to the LDA, using the asymptotically correct potential of van Leeuwen and Baerends (LB94) in the large r region. The performance of our AC-LDA v_{xc} is assessed for the calculation of TD-DFT excitation energies for a large number of excitations, including both valence and Rydberg states, for each of four small molecules: N_2 , CO, CH_2O , and C_2H_4 . The results show a significant improvement over those from either the LB94 or the LDA functionals. This confirms that the DD is indeed an important element in the design of functionals. The quality of TDLDA/LB94 and TDLDA/AC-LDA oscillator strengths were also assessed in what we believe to be the first rigorous assessment of TD-DFT molecular oscillator strengths in comparison with high quality experimental and theoretical values. And a comparison has been given of TDLDA/AC-LDA excitation energies with other TD-DFT excitation energies taken from the literature, namely for the PBE0, HCTH(AC), and TDLDA/SAOP functionals. Insight into the working mechanism of TD-DFT excitation energy calculations is obtained by comparison with Hartree–Fock theory, highlighting the importance of orbital energy differences in TD-DFT. © 2000 American Institute of Physics. [S0021-9606(00)30844-3]

I. INTRODUCTION

A knowledge of electronic excited states is important for many areas of chemistry and molecular physics, including spectroscopy, photochemistry, and the design of optical materials. Theoretical methods that are both accurate and efficient enough for prediction or interpretation of the discrete spectra of the often sizable molecules encountered in problems of practical interest could make a valuable contribution to these areas. Time-dependent density-functional theory (TD-DFT) has recently emerged as a promising method, offering the advantages of a formally well-founded method combined with the good quality results one has come to expect from density functional theory (DFT). The success¹ of time-independent DFT^{2,3} for calculating a variety of ground-state properties to an accuracy which rivals that of considerably more expensive correlated *ab initio* methods is a testimony to the quality of present approximate exchange–

correlation functionals. In TD-DFT, there are additional demands on the functional which become important for high-lying excited states and that are not met by the functionals normally used for molecular applications. This is true even when the time-dependent theory is considered only within the adiabatic approximation, as is done in the present work.

Although the time-dependent local density approximation (TDLDA) has been found to give remarkably good results for low-lying excitation energies,^{4–12} it has also been shown that, in the adiabatic approximation, the TD-DFT ionization threshold lies at minus the highest occupied molecular orbital (HOMO) energy, $-\epsilon_H^F$ (strictly speaking, at $v_{xc}^\infty - \epsilon_H^F$), for any functional F .^{9,13–15} This becomes the true ionization potential, I , in the case of the exact exchange–correlation potential, v_{xc} ,^{16–20} but $-\epsilon_H^F$ is too low (typically by several eV) for almost all present day approximate functionals. We have given an explicit illustration of the serious problem this artifact presents for the TDLDA calculation of higher excitation energies: States between $-\epsilon_H^{LDA}$ and I , in

^{a)}Electronic mail: Mark.Casida@UMontreal.CA

what should be a discrete part of the spectrum, collapse into a continuum.^{13,9}

The value of the HOMO energy is closely related to the asymptotic behavior of the exchange–correlation potential, which is incorrect for almost all present day approximate functionals. A number of approaches have been suggested for correcting the asymptotic behavior of v_{xc} and hence the value of ϵ_H . (See Ref. 13 for a brief survey.) Most of these approaches are more computationally demanding than is the LDA or gradient-corrected functionals, however several gradient-corrected functionals yielding the correct asymptotic behavior and $\epsilon_H \approx -I$ have been proposed.^{21–25} We found that using the van Leeuwen and Baerends (LB94) potential in the self-consistent field (SCF) step combined with the TDLDA for the coupling (denoted TDLDA/LB94) gives a dramatic improvement over the TDLDA for excitation energies above $-\epsilon_H^{\text{LDA}}$, thus confirming that correct asymptotic behavior of v_{xc} is crucial for these high-lying bound excitations.^{9,13} However, some problems still remained. In particular, for the four molecules studied, most of the higher excitation energies were overestimated, though certain excitations out of σ orbitals are substantially too low, and the TDLDA/LB94 does not do quite as well as the TDLDA for the low-lying states. This indicated a need for further improvement of the functional. In a previous paper, we introduced an asymptotic-correction approach to improving the functional.²⁶ The present paper details the reasoning behind our asymptotic-correction concept, and assesses its effect on TD-DFT excitation energies for four small molecules. We also give a discussion, based upon our asymptotically corrected LDA (AC-LDA) calculations, of the difference between the TD-DFT and Hartree–Fock (HF)-based description of excitations.

II. ASYMPTOTIC CORRECTION APPROACH

In this section we give a detailed explanation of our asymptotic-correction approach. It will be useful to distinguish a “bulk region” of the molecule where the density is large enough that it is not significantly affected by the addition or removal of a tiny fraction of an electron, and an “asymptotic region” where only the most diffuse orbital contributes to the density, which is small. The “large r ” region will refer to anything outside the bulk region (so it includes, but is not limited to, the asymptotic region).

Our asymptotic-correction approach is designed to incorporate certain essential features of the exact v_{xc} , namely the effect of the derivative discontinuity in the bulk region and the correct asymptotic behavior and value of ϵ_H , while maintaining the ease of computability of gradient-corrected functionals. We focus on v_{xc} , rather than E_{xc} , because TD-DFT uses the Kohn–Sham orbitals and orbital energies, but not the total energy.

A. Properties of the exact functional

We begin by discussing the relevant properties of the exact v_{xc} , and the effect on v_{xc} of the derivative discontinuity (DD), or of the lack of a DD in approximate functionals. This will then lead to our asymptotic correction scheme.

The DD affects v_{xc} differently in the bulk and asymptotic regions. In the bulk region, the DD is manifested as a (nonzero) constant shift^{16,27}

$$\Delta_{xc} = v_{xc}^+(\mathbf{r}) - v_{xc}^-(\mathbf{r}) \quad (2.1)$$

$$= \left[\left(\frac{\partial E}{\partial N} \right)_v^+ - \left(\frac{\partial E}{\partial N} \right)_v^- \right] - (\epsilon_L - \epsilon_H) \quad (2.2)$$

$$= (I - A) - (\epsilon_L - \epsilon_H), \quad (2.3)$$

where H and L refer, respectively, to the highest occupied and lowest unoccupied molecular orbitals (HOMO and LUMO) of the N -electron system, within a zero-temperature formalism where integer- N quantities are defined as the usual^{19,27,28} limit from the electron-deficient side. The plus and minus superscripts indicate that the derivative is evaluated at $N \pm 0^+$. In contrast to the well-established place of the DD in the theory for infinite systems, the significance of the DD in finite systems has been more controversial, due to questions of consistency between the ensemble theory and fractional occupation number methods of introducing noninteger particle number into DFT,^{29,30} and to lack of recognition of its impact on practical applications (though this is changing). One of us (M.E.C.) has recently derived a Janak-type theorem for the correlated optimized effective potential (OEP)^{20,31} and thence a formula for Δ_{xc} that is consistent with the ensemble theory result (2.3). So the questions of consistency between the ensemble theory and the fractional occupation number results that had been left open by the earlier exchange-only OEP treatment of Krieger, Li, and Iafrate^{32,33} (refs. 37 and 38 contain a more complete development of the Krieger, Li, Iafrate approach to orbital-dependent density-functional theory) and the related work of Levy and Görling³⁴ have been resolved. Thus it is now quite clear that the exact v_{xc} has a DD, whose magnitude in the bulk region is given by Eq. (2.3). The (correlated) OEP-Janak theorem was also used to confirm the well-known but recently contested^{30,35} ensemble theory result^{17,19} that

$$\epsilon_H = \omega_H, \quad (2.4)$$

where ω_H is the first ionization solution of Dyson’s quasiparticle equation. Since the asymptotic form of the exact v_{xc} is¹⁸

$$v_{xc}(\mathbf{r}) \rightarrow -\frac{f_H}{r} + (\epsilon_H - \omega_H), \quad (2.5)$$

where f_H is the occupation of the HOMO, it follows that^{19,36}

$$v_{xc}^\infty \equiv \lim_{r \rightarrow \infty} v_{xc}(\mathbf{r}) = 0. \quad (2.6)$$

It also follows that, in the asymptotic region,

$$v_{xc}^+(\mathbf{r}) \rightarrow -\frac{\delta}{r}, \quad v_{xc}^-(\mathbf{r}) \rightarrow -\frac{1}{r}, \quad (2.7)$$

upon addition or removal of a small fraction, δ , of an electron. So the DD falls off as $1/r$.^{20,32,33,37,38} The fact that the DD is a constant shift in the bulk region but falls off as $1/r$ in the asymptotic region means that it affects the shape of v_{xc} even at fixed particle number.

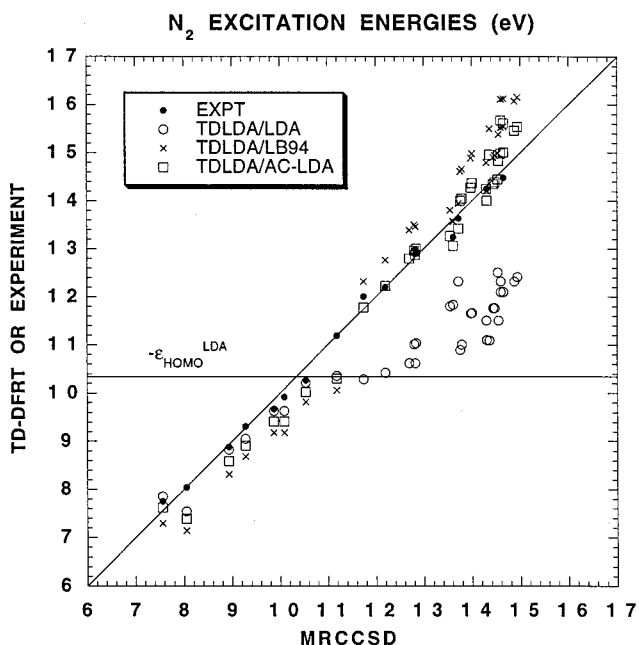


FIG. 1. Comparison of TD-DFT excitation energies calculated using the TDLDA/LDA, TDLDA/LB94, and TDLDA/AC-LDA functionals with the multireference coupled cluster singles and doubles (MRCCSD) results of Ref. 103 for the first 35 transitions (not counting degeneracies) of N_2 . Experimental values taken from Ref. 103 are also shown.

B. Properties of approximate functionals

Perdew and Levy have argued that the properties (2.4) and (2.6) of the exact v_{xc} are altered in the case of an approximate functional which gives a good approximation to the total energy, $E(N)$, but is smooth, lacking the discontinuity in $\partial E/\partial N$ at integer particle number.¹⁶ For such a DD-free (DDF) functional, the value of $(\partial E^{\text{DDF}}/\partial N)$ at integer N must be somewhere in between the values for the true functional at $N+0^+$ and $N-0^+$.¹⁶ Writing this as a weighted average of the “+” and “-” derivatives and using Janak’s theorem gives

$$\epsilon_{\text{HOMO}}^{\text{DDF}} = \left(\frac{\partial E}{\partial N} \right)_v^{\text{DDF}} \cong w \left(\frac{\partial E}{\partial N} \right)_v^{(-)} + (1-w) \left(\frac{\partial E}{\partial N} \right)_v^{(+)} \\ = -[wI + (1-w)A], \quad (2.8)$$

where $0 < w < 1$. For open shell systems, Perdew and Levy argued that w should be $1/2$,¹⁶ and this is consistent with results of calculations on open shell^{16,28,29,39,40} but not closed shell^{39,40} systems, using several approximate functionals. If the corresponding hypothetical v_{xc}^{DDF} has the exact asymptotic form (2.5), then Eq. (2.8) implies^{29,39,40}

$$v_{xc}^{\infty, \text{DDF}} = (1-w)(I-A), \quad (2.9)$$

which is positive. These observations mean that a functional without a DD cannot give simultaneously a good total energy and a $v_{xc} = \delta E_{xc}/\delta \rho$ with the exact properties (2.4)–(2.6).

As an example of what can happen when one tries to correct the asymptotic behavior of the LDA so as to give Eqs. (2.4) and (2.6), without taking into account the DD, consider the LB94 functional. Figure 1(a) of the original LB94 article,²¹ which compares some approximate

exchange–correlation potentials with the exact potential for the beryllium atom, shows that although the LB94 potential tends to the exact potential asymptotically, the two curves are not parallel in the energetically important bulk region. (Parallel curves will lead to the same charge density.) In contrast, the LDA potential is roughly parallel to the exact potential for $r < 6$ bohr (except that it lacks the small blip around $r = 1$ bohr, which is associated with shell structure, and which can be obtained via gradient corrections). This suggests that the LDA charge density should be a good approximation to the true charge density over this range. Thus it appears that the LB94 gradient correction is improving the asymptotic behavior of the potential at the expense of distorting the already pretty good behavior of the LDA potential in the bulk region. This view is consistent with the difficulties of the TDLDA/LB94 for low-lying excitations mentioned in Sec. I, and is borne out by results for other properties as well. In a comparison of the dipole moments for nine molecules, we found that the LB94 gradient correction often leads to a deterioration in the accuracy of the dipole moment.⁴¹ Neumann, Nobes, and Handy³⁹ have arrived at a similar conclusion about the LB94 functional based on their study of optimized geometries and total energies. Furthermore, similar observations have been made about other functionals which attempt to impose the correct asymptotic behavior on the LDA via a gradient correction.^{24,25}

In order to understand more clearly how ignoring the DD leads to distortions in v_{xc} , and to see how this can be rectified, note that the value (2.8) of ϵ_H^{DDF} suggests that v_{xc}^{DDF} lies between the exact v_{xc}^- and v_{xc}^+ in the energetically important bulk region. As discussed in Sec. I, the good results obtained from the LDA and gradient-corrected functionals (GCFs) for properties primarily dependent on the bulk region, as well as explicit calculations of v_{xc} for atoms (see e.g., Refs. 21, 42, 43), suggest that the v_{xc} ’s from these functionals roughly parallel the exact v_{xc} in the bulk region. Consider, therefore, an approximate exchange–correlation potential, v_{xc}^B , which does not have a DD, which roughly parallels $v_{xc}^- || v_{xc}^+$ in the bulk region, and which satisfies $v_{xc}^- < v_{xc}^B < v_{xc}^+$ in this region. If v_{xc}^B continues to be between v_{xc}^- and v_{xc}^+ in the asymptotic region, then $v_{xc}^{B, \infty} = 0$ but v_{xc}^B cannot have the correct asymptotic behavior unless it coincides with v_{xc}^- [see Eq. (2.7)]. For v_{xc}^B to have the correct asymptotic form, it has to parallel (*grasso modo*) the exact v_{xc}^- in the asymptotic region. This means that either $v_{xc}^{B, \infty} > 0$, consistent with Eq. (2.9), but in violation of the exact condition (2.6), or that $v_{xc}^{B, \infty} = 0$ and v_{xc}^B coincides with v_{xc}^- in the asymptotic region. However, if v_{xc}^B coincides with v_{xc}^- in the asymptotic region, but differs from v_{xc}^- by a constant shift in the bulk region, it cannot be parallel to v_{xc}^- over the entire space. This contradiction shows that there must be a distortion in the shape of v_{xc}^B .

C. Shift-and-splice approach

One way to avoid this distortion is to construct a potential that satisfies the properties (2.8) and (2.9) for a DDF functional, instead of the exact conditions (2.4) and (2.6), so that $v_{xc}^B (= v_{xc}^{\text{DDF}}$ in this case) can maintain a constant differ-

ence from v_{xc}^- in both asymptotic and bulk regions. In a remarkable series of papers,^{40,44–48} Tozer, Handy, and co-workers have considered the problem of fitting the parameters in a general gradient-corrected functional to yield, simultaneously, good exchange–correlation energies and a good shape for exchange–correlation potentials, for a given training set of molecules. Consistent with the DDF nature of the gradient-corrected ansatz, they found that a good simultaneous fit of E_{xc} and v_{xc} was only possible by permitting $v_{xc}^\infty > 0$.⁴⁰ They also confirmed that $-\epsilon_H^{DDF} \approx (I+A)/2$ for open-shell molecules, and $-\epsilon_H^{DDF} < I$ more generally.⁴⁰ In addition to the direct computational confirmation of some important physical ideas, these studies resulted in the development of a highly parametrized “semiempirical” functional (the HCTH functional), satisfying the above-mentioned relations for a DDF functional. This gives good total energies, and represents a first attempt to take the DD into consideration in designing functionals.

We take a second approach which is also aimed at avoiding the distortion of v_{xc} , but which satisfies the exact conditions (2.4) and (2.6). Since v_{xc}^B parallels the exact v_{xc}^- in the bulk region, subtracting an appropriate constant shift, Δ , from v_{xc}^B in the bulk region would bring it into line with v_{xc}^- in this region, thus making it consistent with v_{xc}^- in the asymptotic region. At a given particle number, these two ways of avoiding the distortion in v_{xc} that arises from neglect of the DD amount to the same thing. The difference between the resulting v_{xc} 's is just a constant shift (over all space), so the charge densities and excitation energies are identical. However, as will be seen in the following, the second approach builds the DD into v_{xc} in the bulk region. Thus the two v_{xc} 's are different functions of particle number. In addition, the second approach offers the computational convenience of working with potentials that go to zero at infinity. We thus use the second approach.

It remains to construct the desired potential. This requires both a functional which is good in the bulk region and a functional which gives the correct $-1/r$ asymptotic form. Since the very reason v_{xc} needed improvement is that existing GCFs are not simultaneously good in both bulk and asymptotic regions, we use different functionals for the two regions and splice the potentials together. For the bulk region, we need an easy-to-compute approximate v_{xc} that roughly parallels the exact v_{xc} in this region. The LDA or any of the commonly used GCFs can be used for this purpose. In the present work we will use the LDA. The constant shift required to bring v_{xc}^{LDA} into line with the exact potential is given by the difference between ϵ_H^{LDA} and the exact ϵ_H [Eq. (2.4)],

$$\Delta = \epsilon_H^{LDA} - \omega_H. \quad (2.10)$$

In practice, we approximate ω_H by the total energy difference (Δ SCF) ionization potential calculated with the LDA functional, since this is known to give quite reasonable molecular ionization potentials. For the asymptotic region, we need a potential which has the correct asymptotic behavior. In the spliced asymptotic correction proposed over 40 years ago by Latter⁴⁹ for calculations on atoms, he simply used $-1/r$ at large r ,

$$v_{xc}(\mathbf{r}) = \text{Max} \left(v_{xc}^{\text{TFD}}(\mathbf{r}), -\frac{1}{r} \right), \quad (2.11)$$

where v_{xc}^{TFD} is the Thomas–Fermi–Dirac (TFD) potential. This spliced potential does not take into account the effect of the DD. Moreover, using $-1/r$ itself in the large r region is inappropriate for molecules because it would impose spherical symmetry throughout this region. Instead, what is needed for molecular applications is a form for v_{xc} which is a functional of the density in the large r region, so that it correctly reflects the shape of the molecule, and which yields the correct $-1/r$ behavior as $r \rightarrow \infty$. There are a number of functionals which could be used for this purpose.^{21–25} In the present work we will use the LB94 potential,

$$v_{xc}^{\text{LB94}}(\mathbf{r}) = v_{xc}^{\text{LDA}}(\mathbf{r}) - \beta \rho_\sigma^{1/3} \frac{x_\sigma^2}{1 + 3\beta x_\sigma \sinh^{-1} x_\sigma}, \quad (2.12)$$

where $x_\sigma = |\vec{\nabla} \rho_\sigma| / \rho_\sigma^{4/3}$ and β is a parameter obtained by fitting v_{xc}^{LB94} to the exact exchange–correlation potential for the beryllium atom.²¹ (See Ref. 78 for a summary of subsequent work on functionals by van Leeuwen, Gritsenko, Baerends, and co-workers.) This potential takes advantage of the Becke'88⁵⁰ form for the gradient correction for exchange, which was designed to give the correct $-1/r$ asymptotic behavior for the case of exponentially decaying densities found in atomic and molecular systems, but van Leeuwen and Baerends applied this form to correct v_{xc} directly, instead of the exchange energy density.

Our asymptotically corrected LDA potential (AC-LDA) is obtained by combining the shifted v_{xc}^{LDA} in the bulk region with the LB94 potential in the large r region, taking the switchover point between the two potentials to be where they cross,

$$v_{xc}^{\text{AC-LDA}}(\mathbf{r}) = \text{Max}[v_{xc}^{\text{LDA}}(\mathbf{r}) - \Delta, v_{xc}^{\text{LB94}}(\mathbf{r})]. \quad (2.13)$$

This means of determining the switchover point is the same as that used by Latter.⁴⁹ It may result in a discontinuity in the gradient of $v_{xc}^{\text{AC-LDA}}$ at the location of the splice. However, as the potentials used for the two regions are improved, approaching the true v_{xc} , any discontinuity must vanish. In practice, we expect any effect of a discontinuity in the gradient of v_{xc} to be small compared to the impact of improving the overall shape of the potential, for most computed properties. It is conceivable that the two potentials may not cross in some trivial systems (such as the hydrogen atom), but we expect such systems to be the exception rather than the rule. That the two potentials do cross for the molecules considered in the present paper is obvious from the fact that the AC-LDA results are not the same as those from either of its constituent potentials. We have also not ruled out the possibility that recrossing may occur in certain regions (e.g., near nuclei). Nevertheless, we prefer to stick to the simple prescription (2.13), constructed principally to distinguish between bulk and asymptotic potentials, allowing the two potentials to join naturally wherever they may.

This asymptotic-correction concept was first published along with an application of our AC-LDA potential to the TD-DFT calculation of excited states of 1A_1 manifold of formaldehyde.²⁶ We found that our AC-LDA potential made

possible a sufficiently good simultaneous description of valence and Rydberg excitations that TD-DFT, using this potential, was able to describe the avoided crossings resulting from configuration mixing between valence and Rydberg in this historically enigmatic manifold.

Handy and Tozer^{12,51} have subsequently used our asymptotic correction approach to improve upon their semiempirical functional.⁴⁸ The resultant functional is given the name HCTH(AC). They used the Fermi–Amaldi term, $(1/N)\int \rho(\mathbf{r}')/|\mathbf{r}-\mathbf{r}'|d\mathbf{r}$,⁵² for the large r region, as had previously been done by Santamaria,²⁴ and combined this with their semiempirical functional for the bulk region. [References 53 and 54 contain further applications of the Hamprecht–Cohen–Tozer–Handy [HCTH(AC)] functional or a slight variant thereupon.] Their means of performing the shift-and-splice operation differs from ours in that they introduce two additional adjustable parameters, and they shift the large r potential up, leaving $v_{xc} = \delta E_{xc}/\delta\rho$, instead of shifting the bulk-region potential down, $v_{xc} = \delta E_{xc}/\delta\rho - \Delta$, as we do. This is really a very small difference in philosophy which has little impact on actual computations. More important, the fact that they find their semiempirical functional to be inadequate for high-lying excitation energies, but obtain excellent results using it together with the shift-and-splice asymptotic correction approach,^{12,51} provides confirmation of the basic ideas involved in our asymptotic-correction approach.

Note that we have not introduced any adjustable parameters, since both the shift of the LDA potential and the position of the splice are uniquely determined. (Tozer and Handy introduced two new empirical parameters in their adaption of our shift-and-splice procedure.) We use the Vosko, Wilk, and Nusair parametrization of the LDA,⁵⁵ and the value of β determined by van Leeuwen and Baerends for their potential.²¹ It stands to reason that the results could be improved by redetermining β specifically for the AC-LDA rather than using the value for the pure LB94 potential. However, this would muddy the comparison with the pure LB94 results and is not done here.

A novel and noteworthy aspect of our asymptotic correction approach is that the incorporation of the constant shift, Δ , builds the DD into the potential in the bulk region. Since the LDA has no DD (i.e., $v_{xc}^{LDA,+} = v_{xc}^{LDA,-}$), Eq. (2.13) gives for the DD of the AC-LDA potential, in the region where it consists of the shifted LDA,

$$\begin{aligned} \Delta_{xc}^{AC-LDA} &= \Delta^- - \Delta^+ \\ &= (\epsilon_H^{LDA,-} - \omega_H^-) - (\epsilon_H^{LDA,+} - \omega_H^+) \\ &= (\epsilon_H^{LDA} - \omega_H) - (\epsilon_L^{LDA} - \omega_L), \end{aligned} \quad (2.14)$$

since the HOMO of the system with $N+0^+$ electrons is just the LUMO of the N -electron system, both for the LDA and the Dyson orbitals (because neither involves a DD). This is the same as Eq. (2.3) for the exact Δ_{xc} , except that the true Kohn–Sham orbital energy difference ($\epsilon_L - \epsilon_H$) is here approximated by $(\epsilon_L^{LDA} - \epsilon_H^{LDA})$. This is the first v_{xc} that is easily computed from GCFs to include a DD. Although the

OEP, and the Krieger–Li–Iafrate (KLI) approximation thereto, include the DD, these potentials are much more computationally demanding than GCFs.

For completeness, we specify an approximation for the total energy. Since the philosophy of our asymptotic correction approach is to leave the shape of v_{xc}^{LDA} unchanged in the energetically important bulk region and correct it only in the large r region which is relatively unimportant energetically, we simply use the LDA energy expression but evaluate it using the AC-LDA orbitals and orbital energies. Specifically,

$$\begin{aligned} E^{LDA}[\rho^A] &= \sum_i f_i \epsilon_i^A - \int v_{xc}^A(\mathbf{r}) \rho^A(\mathbf{r}) d\mathbf{r} \\ &\quad - \frac{1}{2} \iint \frac{\rho^A(\mathbf{r}_1) \rho^A(\mathbf{r}_2)}{r_{12}} d\mathbf{r}_1 d\mathbf{r}_2 \\ &\quad + E_{xc}^{LDA}[\rho^A], \end{aligned} \quad (2.15)$$

where the ϵ_i^A and ρ^A are solutions of the Kohn–Sham equation with the exchange–correlation potential v_{xc}^A . This is a variational upper bound on the LDA total energy, becoming the LDA total energy when $A = \text{LDA}$. Using this energy expression with $A = \text{AC-LDA}$ gives an approximate AC-LDA energy. Although this does not satisfy the exact condition $v_{xc} = \delta E_{xc}/\delta\rho$ because we use E_{xc}^{LDA} with v_{xc}^{AC-LDA} , it does allow us to check the premise that our asymptotic correction has very little effect on the shape of v_{xc} in the bulk region. Indeed, the only difference between the LDA energy and the “AC-LDA energy” obtained from this expression is due to the change in the shape of v_{xc} . To see this, note that the effect of a purely constant shift cancels out in the first two terms: for $v_{xc}^A = v_{xc}^{LDA} - \Delta$, Eq. (3.15) reduces to the LDA total energy. A comparison between $E^{LDA}[\rho^{LDA}]$ and $E^{LDA}[\rho^{AC-LDA}]$ will be given in Sec. IV A. Aside from this check, the only use that is made of this energy expression in our calculations is as the energy convergence criterion in the SCF step, since the total energy does not enter into the excitation energy calculations.

Although we have presented the specifics of our asymptotic correction approach for correcting the LDA and using the LB94 potential in the asymptotic region, it is clear that the approach is general and could be used to combine the advantages of any potential which gives a good description of the bulk region with any other potential which has the correct asymptotic behavior.

III. COMPUTATIONAL DETAILS

Time dependent density-functional theory (TD-DFT) provides a rigorous extension of the traditional ground stationary state DFT into the time domain, thus allowing the dynamic response of the charge density, and thereby excitation spectra, as well as a number of other dynamic or excited-state properties, to be obtained. The formal underpinnings of TD-DFT are by now well established, and have been reviewed a number of times by Gross and co-workers.^{56–59} Several years ago, we introduced TD-DFT methodology for molecular applications,^{4,13,60,61} which has since been incorporated into a number of major quantum

chemistry programs. Articles covering methodology and algorithms include Refs. 5, 6, 11, 13, 15, 61, and 62.

The TD-DFT calculations in the present paper were performed using version 2 of our program deMon-DynaRho (for “dynamic response of ρ ”).⁶³ This program follows the methodology described in Ref. 61, but differs from version 1 (used in Ref. 4) in that it also incorporates improvements along the lines described in Ref. 13. This is a post-SCF program designed to be used with deMon-KS (for Kohn–Sham)⁶⁴ for the SCF step. The SCF calculations were performed with version 1.2 of the deMon-KS module, to which we added the LB94 and AC-LDA potentials. For both of these functionals, convergence criteria are based on the charge density fitting coefficients and the LDA total energy. The Δ SCF-based excitation energies were calculated according to the traditional prescription,^{65,66} using SCF energies obtained from version 4.0 of deMon-KS,⁶⁷ since this version allows greater control of excited configurations. Computational details, including molecular geometries, basis sets, and grids, are the same as those given in Ref. 9. Briefly, the orbital basis set consists of the Sadlej basis, augmented with additional diffuse functions. The auxiliary basis sets were chosen from the deMon basis set library. (See Ref. 9 for details.)

The slow decay of asymptotically correct exchange–correlation potentials, such as the LB94 and AC-LDA potentials, makes the convergence of auxiliary basis sets more difficult. Experimentation with more diffuse auxiliary basis sets was hampered by SCF convergence problems. Nevertheless, we have made a number of tests to explore this problem. Although we have seen differences between certain auxiliary basis sets produce differences in excitation energies as large as a few tenths of an eV for some states, there are significant variations in the sensitivity of different states to the auxiliary basis. Thus, in view of the large number of states considered in this paper, it is unlikely that incompleteness of the auxiliary basis set used could result in systematic errors large enough to alter our conclusions concerning the relative performance of the LB94 and AC-LDA functionals.

IV. RESULTS

In this section, we assess the performance of our AC-LDA potential for the calculation of excitation spectra. For this purpose, we consider a large number of discrete states, including both valence and Rydberg excitations, for each of four small, well-studied molecules: N₂, CO, CH₂O, and C₂H₄. These molecules may also be considered as prototypes for studying the (n, π^*) and (π, π^*) transitions important for organic photochemistry. Before looking at the excitation energies, we first consider a few ground-state properties in order to confirm that our asymptotic correction scheme is indeed not resulting in any great distortion of the shape of the LDA potential in the bulk region. We then consider the performance of the AC-LDA for excitation energies and make a preliminary assessment for oscillator strengths. The section ends with a discussion of how the physical description of excitations in TD-DFT differs from that in Hartree–Fock (HF)-based theories, in particular the importance of orbital energy differences for TD-DFT.

TABLE I. Effect of LB94 and AC-LDA corrections to v_{xc}^{LDA} on the total energy calculated using the LDA energy expression.

Molecule	Energy relative to the LDA energy (mhartree)	
	LB94	AC-LDA
N ₂	16.03	2.81
CO	15.97	1.34
CH ₂ O	19.12	2.27
C ₂ H ₄	20.08	3.51

A. Ground state properties

We first verify the premise that the asymptotic correction in the AC-LDA has relatively little effect on the shape of the exchange–correlation potential in the bulk region. Since the LDA orbitals minimize the LDA total energy, the increase in the LDA energy when it is evaluated using orbitals from some other functional, A , Eq. (2.15), is a measure of how much the LDA and A orbitals differ in the energetically important region of space. Table I shows that, while the energy evaluated with the LB94 orbitals exceeds that evaluated using the LDA orbitals by 15–20 mhartrees, the AC-LDA orbitals yield an energy only 1–4 mhartree higher than the LDA energy, confirming that the AC-LDA leaves the LDA orbitals largely unchanged over the energetically important part of space.

Table II shows the effect of the AC-LDA and the LB94 on the LDA dipole moment. Here again the impact of our AC-LDA correction on the charge density in the bulk region is seen to be relatively small, changing the LDA dipole moment by at most about a tenth of a debye. For formaldehyde, the AC-LDA and LDA dipole moments are nearly identical, and are close to experiment, while the LB94 value is larger. For CO, the AC-LDA dipole moment is closer to experiment than is the LB94 dipole moment, which itself is an improvement on the LDA dipole moment, though the differences between all three functionals and experiment are small.

Finally, the relatively small effect of the spliced asymptotic correction on the shape of the LDA potential in the bulk region can be seen from the value of $-\epsilon_H^{AC-LDA}$. The $-\epsilon_H$ for all three functionals are compared with LDA Δ SCF and experimental ionization potentials, I , in Table III. First note that the well-known, severe underestimate of I by $-\epsilon_H^{LDA}$ (errors of 4–5 eV for the present molecules) is largely corrected by the LB94 functional. However, the LDA Δ SCF I is significantly closer to experiment than is $-\epsilon_H^{LB94}$ (absolute errors of 0.02–0.26 eV as opposed to 0.3–1.2 eV).

TABLE II. Dipole moments.

	Dipole moment (D)	
	CO	CH ₂ O
LDA	0.25	2.29
LB94	0.17	2.64
AC-LDA	0.14	2.29
Expt.	0.12 ^a	2.33 ^b

^aFrom Ref. 97.

^bFrom Ref. 98.

TABLE III. Vertical first ionization potential and $-\epsilon_H$.

Molecule	$-\epsilon_H$ (eV)			Ionization potential (eV)	
	LDA	LB94	AC-LDA	ΔSCF^a	Expt. ^b
N ₂	10.36	15.90	15.36	15.62	15.60
CO	9.10	14.32	13.78	14.10	14.01
CH ₂ O	6.32	11.78	10.85	10.92	10.88
C ₂ H ₄	6.91	11.89	11.01	10.94	10.68

^aDifference of LDA total energies for the cation and neutral.^bFrom Refs. 99 (N₂ and CO), 100 (CH₂O), and 101 (C₂H₄).

The $\Delta\text{SCF } I$ is used to determine the value of Δ used in the AC-LDA. So if the AC-LDA consisted only of a rigid shift of the LDA potential, $-\epsilon_H^{\text{AC-LDA}}$ would equal the $\Delta\text{SCF } I$. Thus the effect of the spliced asymptotic correction on ϵ_H is seen as the difference between $-\epsilon_H^{\text{AC-LDA}}$ and the $\Delta\text{SCF } I$, which varies from 0.07 to 0.32 eV, for the present molecules. The resulting $-\epsilon_H^{\text{AC-LDA}}$ is in better agreement with experiment than is $-\epsilon_H^{\text{LB94}}$ (errors of 0.03–0.33 vs. 0.30–1.21 eV). This difference is particularly important for formaldehyde and ethylene, where $-\epsilon_H^{\text{LB94}}$ overestimates I by about 1 eV.

The effect of the asymptotic correction can also be seen in terms of the other orbital energies, as illustrated for CH₂O in Table IV. Here $v_{\text{xc}}^{\text{LDA}}$ supports only two bound virtuals above the LUMO, and the higher of these two is already significantly affected by the incorrect asymptotic behavior of

TABLE IV. CH₂O bound orbital energies.

State ^a	Orbital energy (eV)			
	LDA	LB94 ^b	AC-LDA	LDA- Δ^c
12a ₁		-0.179 37	-0.122 67	
5b ₁		-0.274 84	-0.192 62	
11a ₁		-0.551 17	-0.496 05	
5b ₂		-0.721 88	-0.554 36	
4b ₁		-0.880 37	-0.874 91	
10a ₁		-1.058 5	-0.972 59	
1a ₂ (3d _{xy})		-1.214 6*	-1.161 3	
9a ₁ (3d _{z²})		-1.134 1*	-1.161 8	
4b ₂ (3d _{xy})		-1.240 0	-1.209 2	
8a ₁ (3d _{x²-y²})		-2.308 5	-2.063 2	
3b ₁ (3p _x)		-2.378 4	-2.270 4	
3b ₂ (3p _y)		-3.328 9	-2.942 2	
7a ₁ (3p _z)		-3.363 1	-3.188 1	
6a ₁ (3s)	-0.47081	-4.575 7	-4.170 1	-5.07
2b ₁ (π^*)	-2.9821	-8.618 9	-7.580 7	-7.58
	HOMO-LUMO gap			
2b ₂ (n)	-6.3210	-11.781	-10.846	-10.92
1b ₁ (π)	-10.321	-15.838	-14.912	-14.92
5a ₁ (n σ)	-11.123	-16.456	-15.528	-15.52
1b ₂	-12.228	-17.320	-16.586	-16.83
4a ₁	-15.650	-20.735	-19.984	-20.25
3a ₁	-26.634	-31.671	-31.036	-31.23
2a ₁	-269.44	-293.91	-275.03	-274.04
1a ₁	-507.73	-537.70	-512.51	-512.33

^aOrbital symmetries have been assigned according to the 1955 IUPAC recommendations (Ref. 102).^bAn asterisk indicates a change of orbital ordering relative to that of the AC-LDA.^cLDA orbital energies shifted by the difference between $-\epsilon_H^{\text{LDA}}$ and the LDA ΔSCF ionization potential.

$v_{\text{xc}}^{\text{LDA}}$.⁹ Thus the shifted LDA orbital energy, $\epsilon_i^{\text{LDA}} - \Delta$, does not correspond closely to $\epsilon_i^{\text{AC-LDA}}$ for this orbital (a 0.9 eV difference). For the LUMO and the valence orbitals, the $\epsilon_i^{\text{AC-LDA}}$ show the expected small perturbation of the $\epsilon_i^{\text{LDA}} - \Delta$ due to the asymptotic splice. Note that $\epsilon_i^{\text{LDA}} - \Delta > \epsilon_i^{\text{LB94}}$, so $v_{\text{xc}}^{\text{LDA}} - \Delta$ is indeed the potential used in the bulk region, according to Eq. (2.13). And $\epsilon_i^{\text{AC-LDA}}$ is closer to $\epsilon_i^{\text{LDA}} - \Delta$ than to ϵ_i^{LB94} , with differences between $\epsilon_i^{\text{AC-LDA}}$ and $\epsilon_i^{\text{LDA}} - \Delta$ of a couple tenths of eV, for these orbitals. For the core orbitals, where any perturbation of $\epsilon_i^{\text{LDA}} - \Delta$ by the asymptotic splice should be minimal, the $\epsilon_i^{\text{AC-LDA}}$ are within 1 eV of the $\epsilon_i^{\text{LDA}} - \Delta$, whereas the ϵ_i^{LB94} differ by about 20 eV.

All in all, the effect of the spliced asymptotic correction on predominantly bulk region properties is relatively small. We will now turn to an examination of excitation energies, where the long-range behavior of v_{xc} is very important.

B. Excitation energies

We evaluate the performance of our AC-LDA potential for calculating excitation spectra and compare it to that of the LDA and LB94 potentials. In all our calculations, the TDLDA is used to describe the response (i.e., to evaluate the coupling matrix), while the other functionals are used to obtain v_{xc} in the SCF step. This is denoted TDLDA/F, where F is the functional used for the SCF step. Corrections to v_{xc} do not necessarily improve its derivative, $\delta v_{\text{xc}} / \delta \rho$.⁶⁸ In fact, although TDLDA/LB94 static polarizabilities are a significant improvement over the TDLDA/LDA values,^{41,68} we have found that including the LB94 correction in the response (i.e., LB94 instead of TDLDA/LB94) results in a substantial underestimate of the polarizabilities, giving worse results than the TDLDA/LDA.⁴¹ The present use of TDLDA/F allows us to isolate and study the important problem of improving the shape of v_{xc} , as distinct from the question of its derivative.

The results from all three potentials are compared with published single-particle excitation energies from high-quality *ab initio* methods and with experiment. This comparison covers both singlet and triplet states over a fairly wide range of energies (almost up to the ionization potential.) Theory predicts a number of highly excited states which either do not appear to have been observed experimentally or for which accepted experimental excitation energies are not available. For this reason, our primary comparison is against the *ab initio* calculations. The choice of *ab initio* results against which to compare was governed by the desire to use, insofar as possible, a single set of results for each molecule, that would give reasonably accurate values for all the states considered. The selected calculations are in good agreement with experiment. The state-by-state comparison between the results of different calculations was made by identifying the n th state of a given symmetry from one calculation with the n th state of the same symmetry in the other calculation, with the TD-DFT N -electron term symbol being determined according to the procedure described in Ref. 61. For ethylene, only excitations out of the $1b_{3u}(\pi)$ orbital are considered, and the same state-by-state compari-

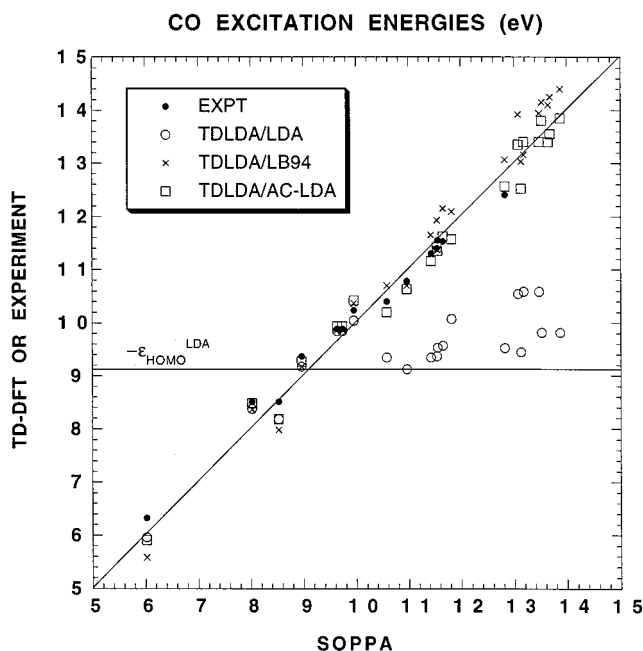


FIG. 2. Comparison of TD-DFT excitation energies calculating using the TDLDA/LDA, TDLDA/LB94, and TDLDA/AC-LDA functionals with the second-order polarization propagator (SOPPA) results of Ref. 104 ($S \neq 1$ results from Table II of that reference) for the first 23 states (not counting degeneracies) of CO. Experimental values taken from Ref. 104 are also shown.

son scheme used for the other molecules is applied to this π -excitation manifold. The σ -excitation manifold of ethylene has been much less studied and will be discussed separately. As was done in our previous paper,⁹ the assignment of excitations to the σ vs π manifold was confirmed by an additional calculation in which all occupied orbitals except the $1b_{3u}(\pi)$ were frozen during the post-SCF step. The results of these comparisons, for the four molecules, are shown in Figs. 1–4. [Time-dependent density-functional response theory (TD-DFRT) and TD-DFT are synonymous in the present context.]

It is immediately evident from Figs. 1–4 figures that, like the TDLDA/LB94, the TDLDA/AC-LDA corrects the disastrous collapse of the TDLDA/LDA excitation energies above $-\epsilon_H^{LDA}$. This is as it should be, since the AC-LDA was designed to correct the asymptotic behavior of v_{xc} and we have already seen that $-\epsilon_H^{AC-LDA}$ are good estimates of the experimental ionization potentials (Table III). It is also apparent that the TDLDA/AC-LDA excitation energies are in significantly better agreement with the experimental and the high-quality *ab initio* results than are the TDLDA/LB94 values. This is further evidenced in Table V where it is seen that the average (over all states) absolute error for the TDLDA/AC-LDA varies from less than half (for ethylene) to two-thirds (for CO) that for the TDLDA/LB94.

The TDLDA/LB94 generally gives excitation energies that are too low below $-\epsilon_H^{LDA}$ and too high above $-\epsilon_H^{LDA}$. The AC-LDA improves on this both below and above $-\epsilon_H^{LDA}$. Below $-\epsilon_H^{LDA}$, TDLDA/AC-LDA moves from the TDLDA/LB94 values back toward the TDLDA/LDA, which does the best of the three. This is consistent with the idea behind the construction of the AC-LDA, namely that, while

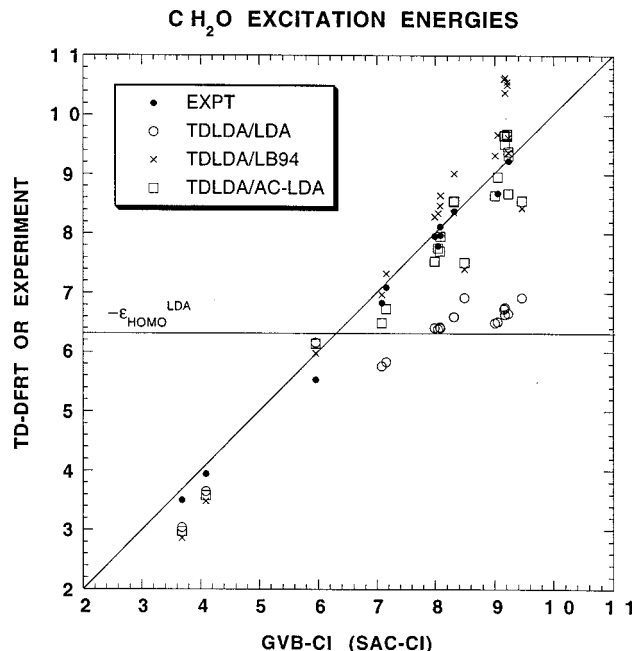


FIG. 3. Comparison of TD-DFT excitation energies calculating using the TDLDA/LDA, TDLDA/LB94, and TDLDA/AC-LDA functionals with the generalized-valence-bond configuration-interaction (GVB-CI) results of Ref. 108 [except for the 1^3B_1 values which are symmetry-adapted cluster configuration interaction (SAC-CI) results from Table III of Ref. 109] for the first 23 states of CH_2O . Experimental values taken from Refs. 105 and 106 are also shown.

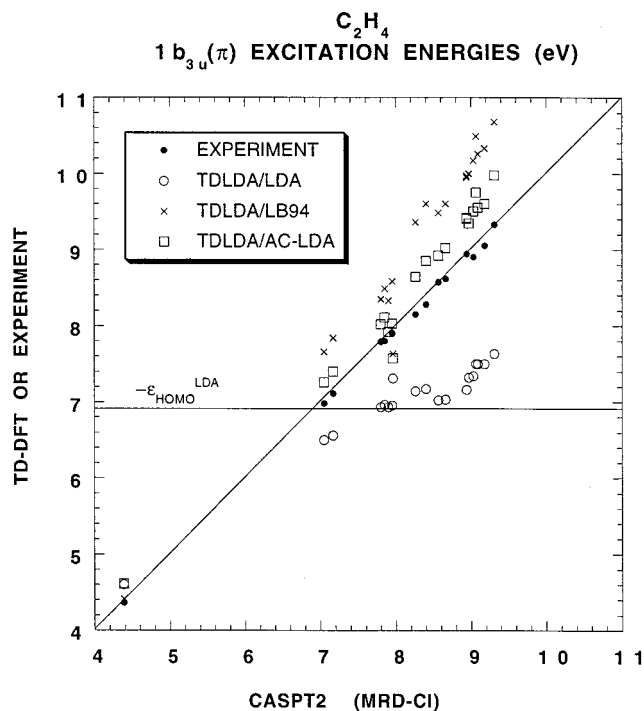


FIG. 4. Comparison of TD-DFT excitation energies calculated using the TDLDA/LDA, TDLDA/LB94, and TDLDA/AC-LDA functionals with the complete-active-space second-order perturbation theory (CASPT2) results of Ref. 107 [except for the $1B_{1u}$ value which is the more accurate multireference doubles configuration interaction (MRDCI) result of Ref. 110] for the first 20 vertical excitation energies out of the $1b_{3u}(\pi)$ orbital of C_2H_4 . Experimental values taken from Ref. 107 are also shown.

TABLE V. Average and maximum errors in TD-DFT excitation energies with respect to the *ab initio* comparison data in Figs. 1–4 (see the figure captions).

	TD-DFT excitation energy errors (eV)							
	Signed error			Absolute error			Maximum error	
	$< -\epsilon_H^{\text{LDA}}$	$> -\epsilon_H^{\text{LDA}}$	All	$< -\epsilon_H^{\text{LDA}}$	$> -\epsilon_H^{\text{LDA}}$	All	$< -\epsilon_H^{\text{LDA}}$	$> -\epsilon_H^{\text{LDA}}$
N ₂								
TDLDA/LDA	-0.23			0.31			0.51	
TDLDA/LB94	-0.67	0.63	0.37	0.67	0.72	0.71	0.91	1.51
TDLDA/AC-LDA	-0.43	0.14	0.02	0.44	0.33	0.35	0.68	1.07
CO								
TDLDA/LDA	-0.01			0.29			0.55	
TDLDA/LB94	-0.11	0.28	0.22	0.38	0.35	0.35	0.55	0.85
TDLDA/AC-LDA	0.08	-0.06	-0.04	0.30	0.24	0.25	0.46	0.61
CH ₂ O								
TDLDA/LDA	-0.29			0.43			0.64	
TDLDA/LB94	-0.47	0.43	0.31	0.48	0.65	0.63	0.82	1.46
TDLDA/AC-LDA	-0.35	-0.12	-0.15	0.47	0.41	0.41	0.71	0.98
C ₂ H ₄								
TDLDA/LDA	0.21			0.21			0.21	
TDLDA/LB94	0.02	0.88	0.84	0.02	0.91	0.87	0.02	1.42
TDLDA/AC-LDA	0.22	0.33	0.32	0.22	0.37	0.36	0.22	0.68

using LB94 to correct the asymptotic behavior, the AC-LDA should distort the LDA less than does the LB94 in the bulk region. The few (three) exceptions to this observed pattern below $-\epsilon_H^{\text{LDA}}$ include two cases where the TDLDA/LB94 does better than the TDLDA/AC-LDA or the TDLDA/LDA, however all three functionals give results within about 0.25 eV of the experimental and high quality *ab initio* results for these two states. Above $-\epsilon_H^{\text{LDA}}$ the TDLDA/LB94 generally overestimates the excitation energies, and the error increases with energy. The TDLDA/AC-LDA generally reduces these values, bringing them into better agreement with the experimental and high quality *ab initio* results.

This is particularly striking in ethylene, where, of the 19 states above $-\epsilon_H^{\text{LDA}}$ in the $1b_{3u}(\pi)$ manifold, 11 are off by an electron volt or more (errors from 1.0 to 1.4 eV) with the TDLDA/LB94 functional. The TDLDA/AC-LDA gives a very marked and systematic improvement, reducing the average error above $-\epsilon_H^{\text{LDA}}$ from 0.91 to 0.37 eV and yielding errors less than 0.5 eV for almost all the states, the only two exceptions being the $2^{1,3}B_{1u}$ (the highest and fourth highest states shown) with errors of 0.67 and 0.68 eV, respectively (still less than half the error of the TDLDA/LB94 for these states). While the TDLDA/AC-LDA is a substantial improvement over the TDLDA/LB94, it still systematically overestimates the excitation energies for C₂H₄. This is partly a reflection of the fact that the LDA Δ SCF ionization potential overestimates the experimental value by 0.26 eV for C₂H₄, in contrast to the LDA Δ SCF ionization potentials for the other molecules which are within 0.1 eV of experiment. An overestimation of the LDA Δ SCF ionization potential increases the size of the shift, Δ , in the AC-LDA, increasing the difference between the energies of the initial orbital, bound in the shifted LDA potential, and the final Rydberg orbital, supported by the long-range behavior of the LB94 potential, thus yielding excitation energies that are too large

(except for excitations to the LUMO, which is largely unaffected by the LB94 part of the AC-LDA potential). As shown in Table VI, replacing the Δ SCF IP with the experimental IP for C₂H₄ leads to little change in the TDLDA/AC-LDA mean absolute deviations (MADs) below $-\epsilon_H^{\text{LDA}}$, but leads to a significant reduction of the TDLDA/AC-LDA MADs above $-\epsilon_H^{\text{LDA}}$, so that they are now similar to the TDLDA/AC-LDA MADs observed for the other three molecules.

In contrast to the extensively studied π -excitation manifold of ethylene, excitations out of the σ system are much less well characterized. Nevertheless, one would expect excitations out of the σ system to be significantly higher in energy than those out of the π bond, and this is consistent with the results of time-dependent Hartree–Fock (TDHF),^{69,70} configuration-interaction singles (CIS),⁷¹ and second-order Møller–Plesset perturbation theory corrected CIS (CIS-MP2)⁷¹ calculations. However, as we pointed out in a previous paper, the TDLDA/LB94 results for the σ excitations are apparently significantly too low.⁹ The TDLDA/AC-LDA does not resolve this problem. A particularly clear example is the $1^{1,3}B_{1g}[1b_{3g}(\pi'_{\text{CH}_2}), 1b_{2g}(\pi^*)]$ singlet–triplet pair, where the TD-DFT differs from the other values by about 2 eV, see Table VII. At the end of Sec. IVE we will show that the problem with this σ excitation arises from significant errors in the orbital energy difference.

The observations we have made for ethylene are also manifested in the results for the other molecules, though in a less dramatic fashion. The TDLDA/AC-LDA markedly improves on the TDLDA/LB94 results. Again, however, the σ excitations which were substantially underestimated by the TDLDA/LB94 (the $1^{1,3}B_{1u}[5a_1(n\sigma), 2b_1(\pi^*)]$ excitations in formaldehyde and the $1^3\Pi_u(C)(2\sigma_u, 1\pi_g)$ excitation in N₂), are not significantly improved by the TDLDA/AC-

TABLE VI. Mean absolute errors for TD-DFT excitation energies using different functionals, below and above minus the LDA HOMO orbital energy ($-\epsilon_H^{\text{LDA}}$, see Table III).

	Mean absolute deviation of TD-DFT excitation energy (eV)					
	From experiment ^a			From theory ^b		
	$< -\epsilon_H^{\text{LDA}}$	$> -\epsilon_H^{\text{LDA}}$	All	$< -\epsilon_H^{\text{LDA}}$	$> -\epsilon_H^{\text{LDA}}$	All
N_2^{h}						
TDLDA/LDA ^c	0.19	1.80	1.05	0.31	1.81	1.11
TD-HCTH/HCTH ^d	0.26	2.13	1.26	0.31	2.14	1.29
TD-PBE0/PBE0 ^e
TDLDA/AC-LDA ^c	0.36	0.25	0.30	0.44	0.29	0.36
TD-HCTH/HCTH(AC) ^d	0.25	0.43	0.35	0.30	0.43	0.37
TDLDA/SAOP ^f	0.11	0.17	0.14	0.24	0.20	0.22
CO^{i}						
TDLDA/LDA ^c	0.28	1.28	1.06	0.25	1.40	1.15
TD-HCTH/HCTH ^d	0.41	1.38	1.17	0.15	1.50	1.21
TD-PBE0/PBE0 ^e	0.43	0.28	0.31	0.18	0.35	0.31
TDLDA/AC-LDA ^c	0.26	0.12	0.15	0.31	0.26	0.27
TD-HCTH/HCTH(AC) ^d	0.37	0.31	0.32	0.12	0.44	0.37
TDLDA/SAOP ^f	0.07	0.09	0.09	0.30	0.25	0.26
$\text{CH}_2\text{O}^{\text{j}}$						
TDLDA/LDA ^c	0.46	1.42	1.10	0.43	1.54	1.17
TD-HCTH/HCTH ^d	0.18	1.55	1.09	0.24	1.67	1.19
TD-PBE0/PBE0 ^e	0.17	0.41	0.33	0.41	0.53	0.49
TDLDA/AC-LDA ^c	0.50	0.27	0.34	0.47	0.38	0.41
TD-HCTH/HCTH(AC) ^d	0.17	0.26	0.23	0.23	0.37	0.33
TDLDA/SAOP ^f	0.41	0.17	0.25	0.19	0.11	0.14
$\text{C}_2\text{H}_4^{\text{k}}$						
TDLDA/LDA ^c	0.24	1.15	1.08	0.21	1.21	1.13
TD-HCTH/HCTH ^d	0.04	1.34	1.24	0.07	1.40	1.30
TD-PBE0/PBE0 ^e	0.44	0.17	0.19	0.47	0.23	0.25
TDLDA/AC-LDA ^c	0.25	0.40	0.39	0.22	0.34	0.33
TDLDA/AC-LDA ^{c,g}	0.25	0.26	0.26	0.22	0.20	0.20
TD-HCTH/HCTH(AC) ^d	0.03	0.05	0.05	0.06	0.07	0.07
TDLDA/SAOP ^f

^aExperimental values for N_2 taken from Ref. 103, for CO from Ref. 104, for CH_2O from Refs. 105 and 106, and for C_2H_4 from Ref. 107.

^bTheoretical values for N_2 are MRCCSD results of Ref. 103, for CO are SOPPA results from Ref. 104, for CH_2O are GVB-CI results from Ref. 108 (except for the 1^3B_1 values which are SAC-CI values from Ref. 109), and for C_2H_4 are CASPT2 results of Ref. 107 (except for the $1B_{1u}$ value which is from the MRDCI calculation of Ref. 110.)

^cTime-dependent local density approximation calculations with or without asymptotic correction at the SCF step. Present work.

^dTime-dependent HCTH calculations with or without asymptotic correction at the SCF step (Ref. 12).

^eTime-dependent PBE0 calculations (Ref. 73).

^fTime-dependent local density approximation calculations using the statistical average of orbital model potential at the SCF step (Ref. 72).

^gShift calculated using the experimental IP instead of the ΔSCF LDA IP.

^hBased on data for 15 N_2 states: $1^3\Sigma_u^+$, $1^3\Pi_g$, $1^3\Delta_u$, $1^1\Pi_g$, $1^3\Sigma_u^-$, $1^1\Sigma_u^-$, $1^1\Delta_u$, $1^3\Pi_u$, $1^3\Sigma_g^+$, $2^1\Sigma_g^+$, $1^1\Sigma_u^+$, $1^1\Pi_u$, $2^1\Pi_u$, $3^1\Pi_u$, $2^1\Sigma_u^+$.

ⁱBased on data for 14 CO states: $1^3\Pi$, $1^3\Sigma^+$, $1^1\Pi$, $1^3\Delta$, $1^3\Sigma^-$, $1^3\Sigma^+$, $1^1\Delta$, $2^3\Sigma^+$, $2^1\Sigma^+$, $3^3\Sigma^+$, $3^1\Sigma^+$, $2^3\Pi$, $2^1\Pi$, $4^1\Sigma^+$.

^jBased on data for 9 CH_2O states: 1^3A_2 , 1^1A_2 , 1^3A_1 , 1^3B_2 , 1^1B_2 , 2^3B_2 , 2^1B_2 , 2^3A_1 , 2^1A_1 .

^kBased on data for 13 C_2H_4 states: 1^3B_{1u} , 1^3B_{3u} , 1^1B_{3u} , 1^3B_{1g} , 1^1B_{1g} , 1^1B_{2g} , 1^3A_g , 2^1A_g , 2^3B_{3u} , 2^1B_{3u} , 3^1B_{3u} , 1^1B_{2u} , 2^1B_{1u} .

LDA. The six highest states in N_2 have errors of 0.9–1.5 eV with the TDLDA/LB94, and, while the TDLDA/AC-LDA yields a substantial improvement, the remaining errors for four of these six states are over 0.4 eV (0.6 eV for two of them, 1.0 eV for the other two). These six states are within 1 eV of the (experimental) ionization potential, and would be expected to be difficult to treat quantitatively with any method, in view of the high density of states, and demands

on the basis set. Nevertheless, the impact of errors in the LB94 potential on the AC-LDA may also play a role. This effect should be most important for high-lying states, where the final orbital is bound by the LB94 part of the potential, and for states where the errors from the TDLDA/LB94 are large. A similar remark can be made for the cluster of states in formaldehyde which are placed above 10 eV by the TDLDA/LB94, though in this case the remaining errors with

TABLE VII. Comparison of ${}^{1,3}B_{1g}[1b_{3g}(\pi'_{\text{CH}_2}),1b_{2g}(\pi^*)]$ excitation energies in C_2H_4 obtained by various methods.

Method	C_2H_4 ${}^{1,3}B_{1g}[1b_{3g}(\pi'_{\text{CH}_2}),1b_{2g}(\pi^*)]$ excitation energies (eV)		
	ω_T	ω_S	$\Delta\epsilon$
TDLDA/LB94	6.59	7.08	6.83
TDLDA/AC-LDA	6.70	7.16	6.92
TDLDA/LDA ^a	6.93	6.98	7.19
ΔSCF	7.13	7.52	7.19
Expt ^b		9.2	
TDHF ^b		9.22	
CIS ^c	8.56	9.28	
CIS-MP2 ^c	8.96	9.31	

^aTDLDA/LDA values have only been included after some hesitation, for the sake of completeness. Since the TDLDA/LDA ω_T and ω_S values exceed the TDLDA ionization threshold at $-\epsilon_H^{\text{LDA}}=6.91$ eV, they cannot be considered as meaningful bound state excitation energies. Furthermore these states are heavily mixed in the TDLDA/LDA calculation with the corresponding $B_{1g}[1b_{3u}(\pi),3b_{2u}(3p_z)]$ transitions, making interpretation doubly difficult.

^bTime-dependent Hartree–Fock calculation and experimental assignment from Ref. 69.

^cConfiguration interaction singles (CIS) with and without a second-order Møller–Plesset correction (Ref. 71).

the TDLDA/AC-LDA are less than 0.5 eV. For CO, the errors in the TDLDA/LB94 are smaller than for the other molecules, and the TDLDA/AC-LDA does remarkably well. For the 14 states for which experimental values are shown, the average (absolute) error for the TDLDA/AC-LDA, compared to experiment, is 0.15 eV, while the average error (versus experiment) of the second-order polarization propagator approximation (SOPPA) calculation against which we compare our results is 0.22 eV, for these same states. For several states the TDLDA/AC-LDA and SOPPA are off in opposite directions, so the average difference between the two, 0.27 eV for these states, is slightly larger than the average error of either calculation. For the states where no experimental value is shown, the TDLDA/AC-LDA and SOPPA results agree to within 0.3 eV for all but one state, where the difference is 0.61 eV. In view of the excellent performance of the TDLDA/AC-LDA versus experiment, we hesitate to attribute too much significance to this one larger difference from the SOPPA results.

C. Comparison with other promising functionals

A few other functionals have emerged very recently which seem especially promising for use in TD-DFT calculations of molecular excitation energies,^{12,72,73} insofar as these seem to provide a balanced treatment of both low- and high-lying molecular excitation energies. A comparison of our TDLDA/AC-LDA excitation energies with those from these other functionals is facilitated by the fact that the same test molecules have often been used in assessing new functionals for use in TD-DFT. Mean absolute deviations (MADs) from experiment and from high quality *ab initio* calculations are summarized in Table VI and will be discussed in the following. The MADs are divided into energies below minus the LDA HOMO energy and above this energy.

This choice of $-\epsilon_H^{\text{LDA}}$ as the dividing point was made in order to have a uniform dividing energy for all functionals. In practice, gradient-corrected functionals typically give about the same value of $-\epsilon_H$ and hybrid values give a slightly higher (but still significantly underestimated) value. Because the results for other functionals are taken from the literature, basis functions, the choice of procedure for assigning states, and other sometimes important details may differ. Also the averages in Table VI are limited to commonly reported excitation energies, which typically are only for experimentally observed states—a significantly smaller number of states than we have reported in this paper.

We first begin with a comparison of excitation energies for functionals with no asymptotic correction. In Table VI, these are the TDLDA/LDA functional, the HCTH functional,⁴⁸ and the hybrid functional consisting of the Perdew–Burke–Ernzerhof (PBE) gradient-corrected functional mixed with Hartree–Fock exchange using 0 adjustable parameters (PBE0 functional)⁷³ (labeled TD-HCTH/HCTH and TD-PBE0/PBE0 in Table VI). The HCTH functional was discussed earlier in this paper (Sec. II C). It is a highly parametrized semiempirical gradient-corrected functional which was simultaneously fit to the total energy and to the exact exchange–correlation potential. All four of the molecules considered here were included in the training set for the parameters of the HCTH functional.⁴⁸ It already contains some effects of the derivative discontinuity insofar as the exchange–correlation potential was fitted to upshifted exact exchange–correlation potentials, so one might expect superior excitation energies to those obtained from the TDLDA/LDA functional. Nevertheless the HCTH functional does eventually go to zero at infinity.⁴⁸ Although this is the case for CH_2O and C_2H_4 below $-\epsilon_H^{\text{LDA}}$, the MADs from experiment (but not from the good *ab initio* theory) are actually smaller for the TDLDA/LDA functional than for the HCTH functional for N_2 and CO below $-\epsilon_H^{\text{LDA}}$. Above $-\epsilon_H^{\text{LDA}}$, both the TDLDA/LDA and HCTH functionals show huge MADs (with the HCTH excitation energies having slightly larger MADs). This means that the way the derivative discontinuity is included in the HCTH exchange–correlation potential is insufficient to correct its erroneous asymptotic behavior.

The PBE0 functional is a hybrid functional based upon the nonempirical PBE generalized gradient approximation⁷⁴ mixed with Hartree–Fock exchange using a nonempirical estimate of 1/4 for the mixing parameter.^{75,76} It is not asymptotically corrected and, for a large enough basis set, PBE0 TD-DFT excitation energies are expected to collapse above $-\epsilon_H^{\text{PBE0}}$ [a bit above $-\epsilon_H^{\text{LDA}}$, but still about 3 eV below the experimental ionization potential (see Table XI of Ref. 73)]. However it is remarkable that calculations with the same augmented Sadlej basis set used in the present article lead to relatively little collapse in excited state energies above $-\epsilon_H$,⁷³ although this collapse is observed for the popular Becke exchange plus Lee–Yang–Parr correlation (BLYP) generalized gradient approximation and B3LYP hybrid functionals⁷³ and (as we have seen) with the TDLDA/LDA functional. Some of this seems to be due to the PBE functional itself,⁷³ perhaps indicating that the shape of the PBE

exchange–correlation potential probably remains correct at larger r than is the case for other functionals.⁷⁷ In an earlier article,⁹ we gave two criteria for reliable TD-DFT excitation energies: (1) the TD-DFT excitation energy should be below $-\epsilon_H$ and (2) the unoccupied orbital into which the excitation occurs should not be too close to the threshold region of the Kohn–Sham effective orbital potential. Typically in the molecules considered here, condition (2) is satisfied for the lowest unoccupied molecular orbital (LUMO) but the second lowest unoccupied orbital, though bound, is often just barely bound. It is interesting to speculate how a small improvement in the description of this orbital could lead to a large improvement of excitation energies around and even above $-\epsilon_H$, provided we only consider excitations which are primarily into this second lowest unoccupied orbital. Such a functional should appear to do better at higher energies than does the TDLDA/LDA, but should not do as well as a true asymptotically corrected functional. In fact, Table VI shows that the asymptotically corrected TDLDA/AC-LDA and HCTH(AC) [labeled TD-HCTH/HCTH(AC)] lead to lower MADs than the PBE0 functional above $-\epsilon_H^{\text{LDA}}$.

Examination MADs of the asymptotically corrected functionals below $-\epsilon_H^{\text{LDA}}$ shows that they are about the same as that found with the corresponding functionals without asymptotic correction, and somewhat larger deviations are seen for the AC-LDA functional than for the HCTH(AC) functional. (The latter point is most likely an indication that Tozer and Handy splice on their asymptotic correction at larger distance than occurs for our AC-LDA functional.) Above $-\epsilon_H^{\text{LDA}}$, the MADs of the asymptotically corrected functionals are, of course, much better than that of their uncorrected counterparts. Surprisingly there is no clear advantage of the HCTH(AC) functional over the TDLDA/AC-LDA functional or vice versa above $-\epsilon_H^{\text{LDA}}$. The TDLDA/AC-LDA MADs for N_2 and CO are smaller, while HCTH(AC) does better for C_2H_4 , and the TDLDA/AC-LDA and HCTH(AC) MADs are similar for CH_2O . As mentioned earlier, part of the reason that the TDLDA/AC-LDA overestimates higher excitation energies for C_2H_4 is because the ΔSCF IP overestimates the experimental IP. TDLDA/AC-LDA C_2H_4 excitation energies which have been recalculated using the experimental IP are also shown the Table VI.

Finally we turn to an approximate functional which is designed to take into account as much as possible the derivative discontinuity of the exact functional, while maintaining ease of computability. This is the statistical averaging of (model) orbital potentials (SAOP) of Gritsenko, Schipper, and Baerends.^{72,78} Its form,

$$v_{xc\sigma}^{\text{SAOP}}(\mathbf{r}) = \sum_i^{\text{occupied}} v_{xc\sigma}^{\text{mod}}[\rho_\sigma, x_\sigma](\mathbf{r}; \epsilon_{H\sigma} - \epsilon_{i\sigma}) \frac{|\psi_{i\sigma}(\mathbf{r})|^2}{\rho_\sigma(\mathbf{r})}, \quad (4.1)$$

contains both an orbital energy dependence, reminiscent of the KLI approximation⁷⁹ to the exact exchange potential, and correct behavior in the asymptotic region. Table VI shows that, for the three molecules where comparison data are available, the TDLDA/SAOP functional does particularly well in predicting TD-DFT excitation energies. In particular, of all the functionals in Table VI, the TDLDA/SAOP exci-

tation energies are in best overall agreement with both experiment and good *ab initio* theory excitation energies for N_2 . For CO , the TDLDA/SAOP excitation energies are in best agreement with experiment, with the TDLDA/AC-LDA excitation energies in second best agreement. However, when compared with good *ab initio* theory excitation energies, the best agreement is found for the HCTH(AC) functional below $-\epsilon_H^{\text{LDA}}$ with the TDLDA/SAOP coming in second best. Above $-\epsilon_H^{\text{LDA}}$, the TDLDA/SAOP is best and the HCTH(AC) functional is second best. Finally in the case of CH_2O , the HCTH(AC) functional appears to be in best agreement with experiment, with the TDLDA/SAOP functional coming in second. This order is inverted when comparison is made with the good *ab initio* theory excitation energies rather than experiment.

Perhaps the best way to summarize the results of our comparison is to note that the TDLDA/AC-LDA is the simplest of all the asymptotically correct functionals shown in Table VI, yet seems to give results comparable to those of more complicated functionals. This is almost a little bit surprising, given that the HCTH(AC) and TDLDA/SAOP functionals are considerably more elaborate. However the extra work put into building these functionals does yield excitation energies which are a bit better than the simple TDLDA/AC-LDA. The good results from the HCTH(AC) functional, which is a more elaborate implementation of our shift-and-splice asymptotic correction concept, further confirms the validity of the shift-and-splice approach to correcting the shape of the exchange–correlation potential.

D. Oscillator strengths

Time-dependent density-functional theory produces not just excitation energies but also oscillator strengths. These are important tools in analyzing the behavior of optical response properties and for spectral assignments. Although TD-DFT spectra (including oscillator strengths) have been calculated, for example, for chlorophyll *a*⁸⁰ and a number of fullerenes,⁸¹ almost no assessment of TD-DFT oscillator strengths has been made in comparison with quantitatively reliable experimental and theoretical values. An exception is the work of Baerends and co-workers,¹⁰ who obtained excellent results (i.e., within 6%) from TD-DFT calculations of helium oscillator strengths using an essentially exact exchange–correlation potential. A comparison of TD-DFT and complete active space self-consistent field corrected by second-order perturbation theory (CASPT2) oscillator strengths has also been presented in some recent work by Roos and co-workers,⁵³ who found overly strong mixing between valence and nearby Rydberg excited states for TD-DFT with the HCTH(AC) functional. Here we make a first quantitative comparison of *molecular* TD-DFT oscillator strengths with reliable experimental, and with TDHF and CI values.

With the TDLDA/LDA functional, most bright states lie above $-\epsilon_{\text{HOMO}}^{\text{LDA}}$ in N_2 , CO , CH_2O , and C_2H_4 , so that the TDLDA/LDA oscillator strength distribution is continuous when it should be discrete. This problem is rectified with asymptotically correct functionals, such as the TDLDA/

TABLE VIII. Comparison of the TDLDA/LB94 and TDLDA/AC-LDA oscillator strengths with experiment and other theoretical values.

State	Oscillator strengths ^a [excitation energies (eV)]				
	TDLDA/LB94	TDLDA/AC-LDA	Expt. ^b	TDHF ^c	CI ^d
	CO				
A ¹ Π	0.136 [7.98]	0.156 [8.18]	0.1762 [~8.4]	0.1705 [8.89]	0.1668
	N ₂				
b' ¹ Σ _u ⁺	0.399 [14.21]	0.420 [14.00]	0.278 [~14.2]	0.15 [15.03]	0.31
c' ¹ Σ _u ⁺	0.307 [13.46]	0.248 [12.87]	0.279 [~12.9]	0.65 [14.34]	0.26
Total ¹ Σ _u ⁺	0.706	0.668	0.557	0.80	0.57
o ¹ Π _u	0.126 [13.96]	0.077 [13.42]	0.080 [~13.6]	...	0.15
c ¹ Π _u	0.148 [13.57]	0.417 [13.06]	0.145 [~13.2]	0.091 [13.91]	0.09
b ¹ Π _u	0.243 [12.90]	0.017 [13.00]	0.243 [~12.8]	0.32 [15.10]	0.41
Total ¹ Π _u	0.517	0.511	0.468	...	0.65
	CH ₂ O				
3 ¹ A ₁	0.144 [9.62]	0.055 [9.38]	0.0238 [~9.0]	0.035 08 [9.54]	0.035 [10.3]
2 ¹ A ₁	0.061 [8.64]	0.071 [7.57]	0.0281 [~8.0]	0.056 94 [8.32]	0.14 [8.90]
Total ¹ A ₁	0.205	0.126	0.0519	0.092 02	0.175
3 ¹ B ₂	0.043 [9.67]	0.044 [8.95]	0.0198 [~8.8]	0.020 41 [9.24]	0.81 [9.97]
2 ¹ B ₂	0.011 [8.47]	0.018 [7.70]	0.0605 [~8.3]	0.038 21 [8.22]	0.15 [8.69]
1 ¹ B ₂	0.070 [7.32]	0.055 [6.73]	0.0413 [~7.3]	0.022 79 [7.39]	0.060 [7.52]
Total ¹ B ₂	0.124	0.117	0.1216	0.081 41	1.02

^aDegeneracy weighted.^bOscillator strengths from Refs. 82 and 84 (CO), Ref. 83 (N₂), and Ref. 85 (CH₂O). (The CO oscillator strength of Ref. 84 has been decreased by 2.5% in accordance with the recommendation on p. 69 of Ref. 82.) Rough experimental energies, estimated from the same references are also indicated.^cTime-dependent Hartree-Fock results for CO: from Table II (energy) and Table III (oscillator strength) of Ref. 104. TDHF results for N₂: from Table 4 (energy) and Table 6 (oscillator strength) of Ref. 87. TDHF results for CH₂O: From Table I of Ref. 111.^dConfiguration interaction results for CO from Table III of Ref. 112. CI results for N₂ from Ref. 113. CI results for CH₂O from Table III of Ref. 114.

LB94 and TDLDA/AC-LDA, so that we are now in a position to be able to expect reasonable oscillator strengths from TD-DFT and to assess their quality.

In order to do so, we have to address the problem of finding good quality data for comparison. Oscillator strengths are less frequently reported in the literature than are excitation energies and are more difficult to obtain accurately, both from theory and from experiment.

Experimental absolute optical oscillator strengths may now be measured with considerable accuracy via dipole (*e, e*) spectroscopy,⁸² in particular avoiding line saturation effects which have plagued optical measurements (see, e.g., Fig. 1 of Ref. 83). Such measurements are not yet widely available for all molecules, but the absolute oscillator strengths of CO,⁸⁴ N₂,⁸³ CH₂O,⁸⁵ and C₂H₄ (Ref. 86) have all been measured in this way. These are vibronic spectra involving overlapping vibrational structure for different electronic transitions which must be assigned and summed over vibrational transitions in order to obtain total oscillator strengths for each electronic transition. This is possible for CO,⁸⁴ N₂,⁸³ and CH₂O,⁸⁵ but apparently not yet for C₂H₄.⁸⁶ Even for CO, a good level of consistency has only been obtained for a single oscillator strength⁸⁴ (compare the poor level of agreement between oscillator strengths measured by different groups given in Table IV with the relatively good level of agreement found in Table 3 of Ref. 84).

Theoretical oscillator strengths may differ in value depending on whether they are calculated in the length, veloc-

ity, or mixed representations. For some methods (e.g., TDHF) these representations are guaranteed to be identical but only in the limit of a sufficiently complete basis set. Differences in results obtained in the different representations represent "error bars" on the theoretical values. To put this in perspective, equation-of-motion oscillator strengths may differ by 30% in the length and velocity distributions when valence triple zeta plus diffuse function quality basis sets are used.⁸⁷ A second problem with theoretical calculations of oscillator strengths is that, in some sense, theoretical methods are better at describing *distributions* of oscillator strength rather than the oscillator strengths of specific transitions. This is particularly clear for methods (e.g., TDHF, SOPPA, TD-DFT) obeying the sum rules

$$\sum_I f_I = N \quad (4.2)$$

and

$$\sum_I \frac{f_I}{\omega_I^2} = \alpha, \quad (4.3)$$

where *N* and *α* are, respectively, the total number of electrons and the static polarizability. Insofar as these sum rules are satisfied, spectral intensity is evidently conserved, but the number of allowed transitions in a spectral region can depend on the description of correlation used. In particular, methods which include two-electron promotions explicitly (e.g., SOPPA) increase the number of allowed transitions

beyond the number produced by methods (e.g., TDHF and TD-DFT) which do not explicitly include two-electron promotions, effectively spreading the fixed spectral intensity over more peaks.

Our TD-DFT oscillator strengths, as well as TDHF and CI oscillator strengths taken from the literature are compared in Table VIII with the accurate experimental values of Brion and co-workers, for states where reliable experimental electronic oscillator strengths are available. Consider first the TDHF and CI results. For the one CO transition given in Table VIII, the CI and TDHF methods give essentially the same oscillator strength. In contrast, the $^1\Sigma_u^+$ states of N_2 are a case where the inclusion of correlation effects beyond the TDHF level is important for the calculation of oscillator strengths, so that the CI results are in markedly better agreement with experiment than are the TDHF results. Correlation effects are evidently less important for the N_2 $^1\Pi_u$ oscillator strengths given in Table VIII. Although the TDHF and CI calculations shown in Table VIII did not use the same basis sets, the same general conclusion was obtained for N_2 in a comparison of TDHF and SOPPA oscillator strengths calculated using identical basis sets.⁸⁷ For CH_2O , the TDHF calculation appears to be in better agreement with experiment than is the CI calculation, but this is presumably more of a question of the difference between the quality of the basis set in the 1990 TDHF study, which was roughly twice as large as the basis set used in the 1977 CI study.

We now turn to our TD-DFT oscillator strengths. These are preliminary in the sense that no attempt was made to use the very complete basis sets needed to satisfy the Thomas–Reiche–Kuhn sum rule [Eq. (4.2)], but the augmented Sadlej basis sets used here are generally adequate for calculating polarizabilities, and hence should give reasonably good intensities for the first several bright states contributing to the sum-over-states representation of the polarizability [Eq. (4.3)]. The first thing to notice is that, with a few exceptions, the TDLDA/LB94 and TDLDA/AC-LDA oscillator strengths are in rough semiquantitative agreement. Restricting ourselves to the cases where the TDLDA/LB94 and TDLDA/AC-LDA functionals are in rough agreement (i.e., CO, the $^1\Sigma_u^+$ states of N_2 , and the 1B_2 states of CH_2O), we see that the level of agreement with experiment is (much like the case with the traditional *ab initio* methods) reasonable but not quantitative. Although it is reassuring that the ordering of the TD-DFT N_2 $^1\Sigma_u^+$ intensities is that of CI rather than TDHF, suggesting the inclusion of important correlation effects in TD-DFT, neither TD-DFT, TDHF, nor CI gives the experimental ordering of 1B_2 CH_2O intensities.

The two cases where the TDLDA/LB94 and TDLDA/AC-LDA oscillator strengths are in qualitative disagreement are the $^1\Pi_u$ states of N_2 and the 1A_1 states of CH_2O . This happens because the two functionals lead to different quasidegeneracies which, in turn, lead to different configuration mixing of nearby states. In the N_2 $^1\Pi_u$ case, the partial sum of intensity over the three $^1\Pi_u$ states is essentially the same for the two functionals, but a redistribution of intensity occurs in going from the TDLDA/LB94 to the TDLDA/AC-LDA functional because of the incorrect quasidegeneracy of the b $^1\Pi_u$ and c $^1\Pi_u$ states with the TDLDA/AC-LDA func-

tional. In this case, the TDLDA/LB94 results are in better agreement with experiment. A similar remixing occurs for the 1A_1 states of CH_2O , but this time the remixing is with nearby Rydberg states not shown in Table VIII. Here the TDLDA/AC-LDA calculation is in better agreement with experiment.

In summary, the quality of the TD-DFT oscillator strengths, with the TDLDA/LB94 and TDLDA/AC-LDA functionals, seems comparable to that of the TDHF and CI results, and while they all give reasonable results, none of them is quantitative.

E. Orbital energy differences

Some previous studies^{10,88,89} using (essentially) exact exchange–correlation potentials have emphasized how well Kohn–Sham orbital energy differences (OEDs) approximate excitation energies for atoms. In this section, we discuss under what conditions OEDs approximate excitation energies for molecules. This understanding makes OEDs a powerful tool for analyzing TD-DFT excitation energies and for identifying underlying problems with functionals.

It is useful to contrast the role of OEDs in DFT with the better known role of OEDs in Hartree–Fock (HF). As is well-known in HF, occupied orbitals are subject to the self-consistent field of the $N-1$ other electrons, while virtual orbitals are subject to the self-consistent field of all N electrons. Thus occupied orbital energies provide, after a change of sign, a first approximation to ionization potentials, while virtual orbital energies, after a change in sign, are a first approximation to electron affinities. Consequently virtual orbitals provide a rather bad approximation to the final (target) orbitals for single-electron excitations, since these orbitals should be subject to the self-consistent field of $N-1$ rather than N electrons. Not only must the virtual orbital undergo extensive relaxation to better describe the target orbital of the excitation process, but we must also somehow reconcile the fact that there are typically many more bound excited states originating from a given occupied orbital than there are bound virtual orbitals (because most molecules have only a few positive electron affinities). The traditional resolution to this dilemma is the static exchange approximation (for a recent review see Ref. 90), which is ultimately based on the improved virtual orbital approach of Hunt and Goddard.^{91,92} In its simplest form, the target orbital ψ_a is allowed to relax to $\tilde{\psi}_a$ in the field of the Koopmans' ion formed by removing an electron from the occupied orbital ψ_i . Assuming that the promotion $\psi_i \rightarrow \tilde{\psi}_a$ occurs without a spin flip, then the excitation energies are

$$\omega = (\tilde{\epsilon}_{a(i \rightarrow a)} - \epsilon_i) \pm [i\tilde{a}|\hat{f}_H|i\tilde{a}], \quad (4.4)$$

where the upper (lower) sign corresponds to the singlet (triplet) excitation energy. Here the integral notation

$$[rs|\hat{f}_H|r's'] = \int \int \psi_r(\mathbf{r})\psi_s(\mathbf{r}) \times \frac{1}{|\mathbf{r}-\mathbf{r}'|} \psi_{r'}(\mathbf{r}')\psi_{s'}(\mathbf{r}') d\mathbf{r} d\mathbf{r}' \quad (4.5)$$

has been used and tildes denote relaxed quantities. Note that the quantity $\tilde{\epsilon}_{a(i\rightarrow a)}$ is not the energy, ϵ_a , of the virtual ψ_a in the ground-state HF calculation. Rather $\tilde{\epsilon}_{a(i\rightarrow a)}$ is the eigenvalue of the Fock operator for the single determinant corresponding to the promotion $\psi_i \rightarrow \tilde{\psi}_a$. In terms of the expectation value,

$$\tilde{\epsilon}_a = \langle \tilde{\psi}_a | \hat{F} | \tilde{\psi}_a \rangle, \quad (4.6)$$

of the HF operator, \hat{F} , for the ground state taken with respect to the relaxed orbital, $\tilde{\psi}_a$, for the excited state,

$$\tilde{\epsilon}_{a(i\rightarrow a)} = \tilde{\epsilon}_a + [i\tilde{a} | \hat{f}_H | i\tilde{a}] - [ii | \hat{f}_H | \tilde{a}\tilde{a}]. \quad (4.7)$$

We see from Eq. (4.4) that

$$\omega_T < \Delta \tilde{\epsilon} < \omega_S, \quad (4.8)$$

where ω_S and ω_T are the singlet and triplet excitation energies, respectively, and $\Delta \tilde{\epsilon} = \tilde{\epsilon}_{a(i\rightarrow a)} - \epsilon_i$. These three values approach each other for Rydberg excitations where $\tilde{\psi}_a$ becomes diffuse. In particular, the singlet–triplet gap is small for Rydberg excitations. However at no point is a simple ground state OED (i.e., $\Delta \epsilon = \epsilon_a - \epsilon_i$, *without the tilde*) a good approximation to an excitation energy.

The situation is markedly different in TD-DFT. Here the occupied and virtual orbitals see the same potential. It follows that the virtual orbitals in DFT can provide a better first approximation to the target orbitals for single excitations than is the case in HF. In the case of the simple orbital promotion, $\psi_i \rightarrow \psi_a$, neglecting all relaxation effects and configuration mixing (other than spin symmetrization), the TD-DFT excitation energies are given (after the formulas are appropriately linearized) by^{13,61}

$$\omega = (\epsilon_a - \epsilon_i + [ia | \hat{f}_H + \hat{f}_{xc}^{\uparrow,\downarrow} | ia]) \pm [ia | \hat{f}_H + \hat{f}_{xc}^{\uparrow,\downarrow} | ia], \quad (4.9)$$

where the upper (lower) sign gives the singlet (triplet) excitation energy and

$$[rs | \hat{f}_{xc}^{\sigma,\tau} | r's'] = \int \int \psi_r(\mathbf{r}) \psi_s(\mathbf{r}) \times \frac{\delta v_{xc}^{\sigma}(\mathbf{r})}{\delta \rho_{\tau}(\mathbf{r}')} \psi_{r'}(\mathbf{r}') \psi_{s'}(\mathbf{r}') d\mathbf{r} d\mathbf{r}'. \quad (4.10)$$

The approximation (4.9) is expected to break down in the presence of significant charge transfer during the excitation since this will lead to important orbital relaxation effects. It will also break down in the presence of significant configuration mixing. This is the case for the $\pi \rightarrow \pi^*$ spatial multiplets (Σ^+ , Δ , and Σ^-) in N_2 for symmetry reasons⁴ and for the $^1(\pi, \pi^*)$ excitation in formaldehyde which mixes strongly with nearby transitions of Rydberg character.^{26,93} However TD-DFT excitations are more often dominated by a single orbital promotion than is the case in CIS (and many other HF-based methods) because relaxation of the HF virtuals is manifested as configuration mixing. And Eq. (4.9) does hold for transitions dominated by a single promotion when configuration mixing is of the simple singlet–triplet type.

It is interesting to make a more detailed comparison between the HF expressions (4.4) and (4.7) and the TD-DFT

equation (4.9). The form of the two equations differs only by replacing unrelaxed (ψ_i , ϵ_i , ψ_a , ϵ_a) DFT quantities with the appropriate unrelaxed (ψ_i , ϵ_i) and relaxed ($\tilde{\psi}_a$, $\tilde{\epsilon}_a$) Hartree–Fock quantities, and making the following substitutions:

$$[ia | \hat{f}_{xc}^{\uparrow,\downarrow} | ia] \rightarrow 0, \quad (4.11)$$

$$[ia | \hat{f}_{xc}^{\uparrow,\downarrow} | ia] \rightarrow -[ii | \hat{f}_H | \tilde{a}\tilde{a}]. \quad (4.12)$$

The first of these substitutions follows naturally from the fact that $\hat{f}^{\uparrow,\downarrow} = \hat{O}$ in exchange-only DFT. The second is related to the fact that the Coulomb integrals in TDHF arise from the response of the exchange part of the HF SCF.⁶¹

Returning to DFT (with exchange and correlation), examination of the relative signs and sizes of the integrals in Eq. (4.9) leads to

$$\omega_T < \Delta \epsilon < \omega_S, \quad (4.13)$$

where $\Delta \epsilon = \epsilon_a - \epsilon_i$ (i.e., the *unrelaxed* orbital energy difference). Once again, for Rydberg orbitals, the singlet–triplet splitting will become small, but now the OED, which remains between the singlet and triplet excitation energy, becomes a good approximation for $\omega_T \cong \omega_S$, consistent with previous empirical observations.^{10,88,89} This is in contrast to the Hartree–Fock case where the simple OED is not a good approximation to an excitation energy. A simple consequence of the observation that the OED is a good approximation for Rydberg excitation energies in TD-DFT is that a sufficiently exact exchange–correlation potential must bind a large number of virtual orbitals in order to describe the expected manifold of Rydberg excitations. We have already seen that this is the case with the LB94 and AC-LDA potentials (Table IV). Table IX illustrates, for formaldehyde, that the OEDs lie consistently between or very close to the singlet and triplet TD-DFT excitation energies for the TDLDA/LB94 and TDLDA/AC-LDA functionals, and that ω_S , ω_T , and $\Delta \epsilon$ all approach each other as the Rydbergs become more diffuse at higher energies. Equation (4.13) is not applicable in the case of strong configuration mixing. Since strong mixing occurs in the case of the $^1A_1[1b_1(\pi), 2b_1(\pi^*)]$ and $^1A_1[2b_2(n), 4b_2(3d_{yz})]$ excitation energies in formaldehyde,^{26,93} the values shown in Table IX for these excitation energies are simply diabatic estimates reconstructed from the adiabatic curves, in order to associate an excitation energy with these orbital promotions. Strong configuration mixing is also why $\omega_S < \omega_T$ for the $B_1[2b_2(n), 1a_2(3d_{xy})]$ transition with the TDLDA/AC-LDA functional. Note that although Eq. (4.13) also holds for valence excitations, the OED is not a particularly good estimate of valence excitation energies because the singlet–triplet splitting is large for these excitations.

Table IX also shows that much of the difference in behavior between the TDLDA/LB94 and TDLDA/AC-LDA excitation energies, as well as between both of these and the *ab initio* results, can be explained by the LB94 and AC-LDA OEDs. This is particularly evident at higher energies where the LB94 OEDs are too high compared with the corresponding singlet and triplet excitation energies from experiment and high-quality *ab initio* calculations. Here the AC-LDA

TABLE IX. Comparison of orbital energy differences with corresponding singlet and triplet vertical excitation energies for formaldehyde. Note that the correspondence is more rigorous in some cases than in others. In particular, substantial mixing occurs between the ${}^1A_1[1b_1(\pi),2b_1(\pi^*)]$ and ${}^1A_1[2b_2(n),4b_2(3d_{yz})]$ states (see the text).

Transition	CH ₂ O excitation energies (eV)							
	GVB-CI (SAC-CI) ^a		TDLDA/LB94			TDLDA/AC-LDA		
	ω_T	ω_S	ω_T	ω_S	$\Delta\epsilon$	ω_T	ω_S	$\Delta\epsilon$
Rydberg								
$B_2[2b_2(n),9a_1(3d_{z^2})]$	9.16	9.17	10.61	10.63	10.65	9.65	9.66	9.68
$B_1[2b_2(n),1a_2(3d_{xy})]$	9.21	9.21	10.51	10.56	10.57	9.51	9.38	9.68
$A_1[2b_2(n),4b_2(3d_{yz})]$	9.17	9.23	10.38	...	10.54	9.64	~10.1	9.64
$B_2[2b_2(n),8a_1(3d_{x^2-y^2})]$	9.01	9.05	9.32	9.67	9.47	8.64	8.95	8.78
$A_2[2b_2(n),3b_1(3p_x)]$	8.31	8.32	9.37	9.36	9.40	8.54	8.55	8.58
$A_1[2b_2(n),3b_2(3p_y)]$	8.05	8.09	8.34	8.64	8.45	7.55	7.95	7.90
$B_2[2b_2(n),7a_1(3p_z)]$	7.99	8.08	8.28	8.47	8.42	7.53	7.70	7.66
$B_2[2b_2(n),6a_1(3s)]$	7.08	7.16	6.97	7.32	7.21	6.49	6.73	6.68
Valence								
$B_1[5a_1(\sigma),2b_1(\pi^*)]$	8.49	9.46	7.40	8.43	7.84	7.51	8.55	7.95
$A_1[1b_1(\pi),2b_1(\pi^*)]$	5.96	...	5.98	~9.	7.21	6.14	~9.6	7.33
$A_2[2b_2(n),2b_1(\pi^*)]$	3.68	4.09	2.86	3.48	3.16	2.97	3.58	3.26

^aGeneralized-valence-bond configuration-interaction (GVB-CI) results of Ref. 108 (${}^1,{}^3B_1[5a_1(\sigma),2b_1(\pi^*)]$) values are symmetry-adapted cluster configuration interaction (SAC-CI) results from Table III of Ref. 109.)

OEDs are lower, in better agreement with the experimental data and *ab initio* results.

We can also use Eq. (4.13) to throw some light on a problem previously mentioned in Ref. 9 for the TDLDA/LB94 functional. Namely, that some of the excitations out of the σ system in C₂H₄ appear to be significantly underestimated. A particularly clear example is given by the ${}^{1,3}B_{1g}[1b_{3g}(\pi'_{CH_2}),1b_{2g}(\pi^*)]$ excitations which transfer electrons from a π^* -like orbital (π'_{CH_2}) made up (loosely speaking) of out-of-phase combinations of the four CH σ bonds to the familiar out-of-plane π^* orbital. These excitations appear as the second and third lowest excitations in our TDLDA/LB94 and TDLDA/AC-LDA calculations at 6.5–7.5 eV, even though chemical intuition, TDHF,⁶⁹ CIS,⁷¹ and CIS-MP2⁷¹ calculations would place them at a higher energy. Indeed an experimentally observed transition at 9.2 eV has been assigned as the ${}^1B_{1g}[1b_{3g}(\pi'_{CH_2}),1b_{2g}(\pi^*)]$ transition on the basis of TDHF calculations.⁶⁹ The problem with the TDLDA/LB94 and TDLDA/AC-LDA energies for these two excitations can be traced to the OED. From Table VII, we see that $\Delta\epsilon$ satisfies Eq. (4.13), as expected. However, supposing the true triplet excitation energy to be about 9 eV, all the functionals considered here give $\Delta\epsilon$ about 2 eV below the estimated “true” triplet energy, resulting in correspondingly large errors in the TD-DFT excitation energies for these states. Substantial improvement in the TD-DFT results for these states will thus require improving the functional to yield $\Delta\epsilon$ between the true ω_T and ω_S .

Interestingly, the same problem is also present for Δ SCF calculations of these two excitation energies (Table VII). This may seem surprising, since Δ SCF excitation energies are obtained as total energy differences, rather than via a response calculation using orbital energies. However this can be understood using the simple two-level picture. The Δ SCF excitation energies are then given^{13,61} by

$$\omega = \epsilon_a^{\text{TOM}} - \epsilon_i^{\text{TOM}} \pm [aa|\hat{f}_{xc}^{\uparrow,\downarrow} - \hat{f}_{xc}^{\uparrow,\uparrow}|ii], \quad (4.14)$$

where the upper (lower) sign corresponds to the singlet (triplet) excitation energy and

$$\epsilon_a^{\text{TOM}} = \epsilon_a + \frac{1}{2}([aa|\hat{f}_H + \hat{f}_{xc}^{\uparrow,\uparrow}|aa] - [ii|\hat{f}_H + \hat{f}_{xc}^{\uparrow,\uparrow}|aa]), \quad (4.15)$$

$$\epsilon_i^{\text{TOM}} = \epsilon_i + \frac{1}{2}([aa|\hat{f}_H + \hat{f}_{xc}^{\uparrow,\uparrow}|ii] - [ii|\hat{f}_H + \hat{f}_{xc}^{\uparrow,\uparrow}|ii]),$$

are linearized forms of the orbital energies in Slater’s transition orbital method, where half an electron is excited from ψ_i to ψ_a without changing spin. The centroid of the singlet–triplet splitting is given by

$$\epsilon_a^{\text{TOM}} - \epsilon_i^{\text{TOM}} = \epsilon_a - \epsilon_i + \frac{1}{2}[\Delta\rho_{i \rightarrow a}|\hat{f}_H + \hat{f}_{xc}^{\uparrow,\uparrow}|\Delta\rho_{i \rightarrow a}], \quad (4.16)$$

where $\Delta\rho_{i \rightarrow a}(\mathbf{r}) = |\psi_a(\mathbf{r})|^2 - |\psi_i(\mathbf{r})|^2$ is effectively a charge transfer term.^{94,95} From Table VII, this charge transfer term is seen to be small (i.e., about 0.14 eV) for the $B_{1g}[1b_{3g}(\pi'_{CH_2}),1b_{2g}(\pi^*)]$ transitions, so that Eq. (4.13) also holds to a first approximation in the Δ SCF method, i.e., the OED lies between the Δ SCF singlet and triplet excitation energies. We again see that the OED is too small, relative to the estimated value for the “true” triplet excitation energy, so the fundamental problem with the ${}^{1,3}B_{1g}[1b_{3g}(\pi'_{CH_2}),1b_{2g}(\pi^*)]$ excitation energies is once again seen to be a functional which underestimates the orbital energy difference. A by-product of this discussion is the suggestion that the Δ SCF method contains a charge transfer term which may be important for a correct description of some excitations. This may or may not also be present in TD-DFT, depending on the functionals used. The problem of how explicitly to incorporate this as a charge transfer correction in TD-DFT is discussed elsewhere.^{94–96}

V. CONCLUSION

In this paper we have presented the detailed reasoning behind our novel asymptotic-correction approach to improving v_{xc} that was introduced in a previous paper,²⁶ and we have assessed the performance of our asymptotically corrected potential for calculating excitation energies of four small molecules. We have shown, in some detail, how correcting the asymptotic behavior of v_{xc} without taking the derivative discontinuity into account leads to a distortion of the shape of v_{xc} . Since the correct asymptotic behavior of v_{xc} is crucial for a correct description of high-lying excitations, our approach was designed to compensate for the lack of a DD in the LDA and gradient-corrected functionals. This is done by shifting the LDA (or GCF) v_{xc} down by a constant $=\epsilon_H^{LDA} - \omega_H$ (where $-\omega_H$ is approximated by the Δ SCF ionization potential), in the bulk region. The resulting shifted potential is then spliced onto an asymptotically correct potential, LB94 in the present paper, in the large r region, without introducing any adjustable parameters. This builds the DD into v_{xc} in the bulk region, and it was the first potential to do so while maintaining the ease of computation of the GCFs. The asymptotically corrected LDA (AC-LDA) thus obtained gives significantly better excitation energies than do either of its constituent potentials (LDA or LB94).

The quality of TDLDA/LB94 and TDLDA/AC-LDA oscillator strengths were also assessed in what we believe to be the first rigorous assessment of TD-DFT molecular oscillator strengths in comparison with high quality experimental and theoretical values. And a comparison has been given of TDLDA/AC-LDA excitation energies with other TD-DFT excitation energies taken from the literature, namely for the PBE0, HCTH(AC), and TDLDA/SAOP functionals.

Finally, we have provided an in-depth explanation of how TD-DFT describes excitation energies, which differs significantly from the description via TDHF or other HF-based theories. When a v_{xc} with the correct asymptotic behavior is used, the DFT effective potential binds a large number of virtual orbitals. Thus, not only do occupied orbitals and virtuals see the same effective potential in DFT, but the relevant virtuals are bound. This makes single orbital promotions a much better approximation to excitations in DFT than in HF-based theories. In HF, significant configuration mixing is required to describe the relaxation necessary to produce a bound excited (final) state orbital from the unbound virtuals. We have shown that the primary differences between TD-DFT and TDHF are this much greater role of relaxation in TDHF, and the replacement of exchange-correlation terms in TD-DFT with TDHF terms associated with the exchange part of the SCF. We have also shown that TD-DFT orbital energy differences (OEDs) should lie roughly between the corresponding singlet and triplet excitation energies, except where there is strong configuration mixing. This explains the previous empirical observation^{10,88,89} that DFT OEDs provide a good approximation to excitation energies for atoms. Another consequence is that much of the behavior of TD-DFT excitation energies can be explained simply on the basis of OEDs, so the orbital energies generated by the functional used in the initial SCF step of a TD-

DFT excitation energy calculation are critical. As we have seen, this is the origin of the difficulties with certain σ excitations in ethylene. Interestingly, we have also demonstrated that problems stemming from errors in the orbital energy differences are also present in the traditional Δ SCF-based approach to molecular excitation energies in DFT.

Several specific areas where functionals need improvement have been highlighted in this paper. These include the proper melding of the DD and asymptotic behavior, the importance of improving orbital energies, and the possibility that charge transfer effects should be explicitly incorporated into TD-DFT. These considerations are of broad importance and work along these lines is expected to impact not only on calculations of excitation energies, but also on other properties calculated by TD-DFT, as well as static ground-state properties obtained from DFT.

ACKNOWLEDGMENTS

M.E.C. would like to thank Kim Casida for comments on a draft of the manuscript. Professor C. E. Brion is thanked for comments on Sec. IV D. Financial support through grants from the Natural Sciences and Engineering Research Council (NSERC) of Canada and the Fonds pour la formation des chercheurs et l'aide à la recherche (FCAR) of Québec is gratefully acknowledged.

- ¹W. Koch and M. C. Holthausen, *A Chemist's Guide to Density Functional Theory* (Wiley-VCH, New York, 2000).
- ²P. Hohenberg and W. Kohn, *Phys. Rev.* **136**, B864 (1964).
- ³W. Kohn and L. J. Sham, *Phys. Rev.* **140**, A1133 (1965).
- ⁴C. Jamorski, M. E. Casida, and D. R. Salahub, *J. Chem. Phys.* **104**, 5134 (1996).
- ⁵R. Bauernschmitt and R. Ahlrichs, *Chem. Phys. Lett.* **256**, 454 (1996).
- ⁶R. Bauernschmitt, M. Häser, O. Treutler, and R. Ahlrichs, *Chem. Phys. Lett.* **294**, 573 (1997).
- ⁷M. Petersilka and E. K. U. Gross, *Int. J. Quantum Chem., Symp.* **30**, 181 (1996).
- ⁸M. Petersilka, U. J. Gossmann, and E. K. U. Gross, *Phys. Rev. Lett.* **76**, 1212 (1996).
- ⁹M. E. Casida, C. Jamorski, K. C. Casida, and D. R. Salahub, *J. Chem. Phys.* **108**, 4439 (1998).
- ¹⁰S. J. A. van Gisbergen, F. Kootstra, P. R. T. Schipper, O. V. Gritsenko, J. G. Snijders, and E. J. Baerends, *Phys. Rev. A* **57**, 2556 (1998).
- ¹¹R. E. Stratmann, G. E. Scuseria, and M. J. Frisch, *J. Chem. Phys.* **109**, 8218 (1998).
- ¹²D. J. Tozer and N. C. Handy, *J. Chem. Phys.* **109**, 10180 (1998).
- ¹³M. E. Casida, in *Recent Developments and Applications of Modern Density Functional Theory, Theoretical and Computational Chemistry*, edited by J. M. Seminario (Elsevier Science, Amsterdam, 1996), Vol. 4, p. 391.
- ¹⁴A. Zangwill and P. Soven, *Phys. Rev. A* **21**, 1561 (1980).
- ¹⁵G. D. Mahan and K. R. Subbaswamy, *Local Density Theory of Polarizability* (Plenum, New York, 1990).
- ¹⁶J. P. Perdew and M. Levy, *Phys. Rev. Lett.* **51**, 1884 (1983).
- ¹⁷J. P. Perdew, R. G. Parr, M. Levy, and J. L. Balduz, *Phys. Rev. Lett.* **49**, 1691 (1982).
- ¹⁸C. O. Almbladh and U. von Barth, *Phys. Rev. B* **31**, 3231 (1985).
- ¹⁹J. P. Perdew and M. Levy, *Phys. Rev. B* **56**, 16021 (1997).
- ²⁰M. E. Casida, *Phys. Rev. B* **59**, 4694 (1999).
- ²¹R. van Leeuwen and E. J. Baerends, *Phys. Rev. A* **49**, 2421 (1994).
- ²²P. Jemmer and P. J. Knowles, *Phys. Rev. A* **51**, 3571 (1995).
- ²³A. Lembarki, F. Rogemond, and H. Chermette, *Phys. Rev. A* **52**, 3704 (1995).
- ²⁴R. Santamaria, *Int. J. Quantum Chem.* **61**, 891 (1997).
- ²⁵H. Chermette, A. Lembarki, H. Razafinjanahary, and F. Rogemond, *Adv. Quantum Chem.* (to be published).
- ²⁶M. E. Casida, K. C. Casida, and D. R. Salahub, *Int. J. Quantum Chem.* **70**, 933 (1998).

- ²⁷ L. J. Sham and M. Schlüter, Phys. Rev. Lett. **51**, 1888 (1983).
- ²⁸ J. P. Perdew, in *Density-Functional Methods in Physics*, edited by R. M. Dreizler and J. da Providencia [NATO ASI Ser., Ser. B **123**, 265 (1985)] (Plenum, New York, 1985), p. 265.
- ²⁹ V. Russier, Phys. Rev. B **45**, 8894 (1992).
- ³⁰ L. Kleinman, Phys. Rev. B **56**, 12042 (1997).
- ³¹ M. E. Casida, Phys. Rev. A **51**, 2005 (1995).
- ³² J. B. Krieger, Y. Li, and G. J. Iafrate, Phys. Rev. A **146**, 256 (1990).
- ³³ J. B. Krieger, Y. Li, and G. J. Iafrate, Phys. Rev. A **148**, 470 (1990).
- ³⁴ M. Levy and A. Görling, Phys. Rev. A **53**, 3140 (1996).
- ³⁵ L. Kleinman, Phys. Rev. B **56**, 16029 (1997).
- ³⁶ M. Levy, J. P. Perdew, and V. Sahni, Phys. Rev. A **30**, 2745 (1984).
- ³⁷ J. B. Krieger, Y. Li, and G. J. Iafrate, in *Density Functional Theory*, edited by E. K. U. Gross and R. M. Dreizler (Plenum, New York, 1995), p. 191.
- ³⁸ J. B. Krieger, Y. Li, and G. J. Iafrate, Phys. Rev. A **46**, 5453 (1992).
- ³⁹ R. Neumann, R. H. Nobes, and N. C. Handy, Mol. Phys. **87**, 1 (1996).
- ⁴⁰ D. J. Tozer and N. C. Handy, J. Chem. Phys. **108**, 2545 (1998).
- ⁴¹ M. Castro, M. E. Casida, C. Jamorski, and D. R. Salahub (unpublished).
- ⁴² C.-O. Almbladh and A. C. Pedroza, Phys. Rev. A **29**, 2322 (1984).
- ⁴³ C. J. Umrigar and X. Gonze, in *High Performance Computing and its Application to the Physical Sciences*, edited by D. A. Browne *et al.* (World Scientific, Singapore, 1993), p. 43.
- ⁴⁴ D. J. Tozer, N. C. Handy, and W. H. Green, Chem. Phys. Lett. **273**, 183 (1997).
- ⁴⁵ G. K-L. Chan, D. J. Tozer, and N. C. Handy, J. Chem. Phys. **107**, 1536 (1997).
- ⁴⁶ D. J. Tozer and N. C. Handy, J. Phys. Chem. A **102**, 3162 (1998).
- ⁴⁷ N. C. Handy and D. J. Tozer, Mol. Phys. **94**, 707 (1998).
- ⁴⁸ F. A. Hamprecht, A. Cohen, D. Tozer, and N. C. Handy, J. Chem. Phys. **109**, 6264 (1998).
- ⁴⁹ R. Latter, Phys. Rev. **99**, 510 (1955).
- ⁵⁰ A. D. Becke, Phys. Rev. A **38**, 3098 (1988).
- ⁵¹ N. C. Handy and D. J. Tozer, J. Comput. Chem. **20**, 106 (1999).
- ⁵² E. Fermi and E. Amaldi, Mem. Acc. Ital. **6**, 117 (1934).
- ⁵³ D. J. Tozer, R. D. Amos, N. C. Handy, B. O. Roos, and L. Serrano-Andrés, Mol. Phys. **97**, 859 (1999).
- ⁵⁴ Z.-L. Cai, D. J. Tozer, and J. R. Reimers, J. Chem. Phys. (submitted).
- ⁵⁵ S. H. Vosko, L. Wilk, and M. Nusair, Can. J. Phys. **58**, 1200 (1980).
- ⁵⁶ E. K. U. Gross and W. Kohn, Adv. Quantum Chem. **21**, 255 (1990).
- ⁵⁷ E. K. U. Gross, C. A. Ullrich, and U. J. Gossmann, in *Density Functional Theory*, edited by E. K. U. Gross and R. M. Dreizler [NATO ASI Series 1994], p. 149.
- ⁵⁸ E. K. U. Gross, J. F. Dobson, and M. Petersilka, in *Density Functional Theory*, edited by R. F. Nalewajski, Topics in Current Chemistry, Springer Series Vol. 81 (Springer, Heidelberg, 1996), p. 81.
- ⁵⁹ K. Burke and E. K. U. Gross, in *Proceedings of the Tenth Chris Engelbrecht Summer School in Theoretical Physics*, edited by D. Joubert (Springer, Berlin, 1997).
- ⁶⁰ M. E. Casida, C. Jamorski, F. Bohr, J. Guan, and D. R. Salahub, in *Theoretical and Computational Modeling of NLO and Electronic Materials*, edited by S. P. Karna and A. T. Yeates (American Chemical Society, Washington, DC, 1996), p. 145.
- ⁶¹ M. E. Casida, in *Recent Advances in Density Functional Methods, Part I*, edited by D. P. Chong (World Scientific, Singapore, 1995), p. 155.
- ⁶² S. J. A. van Gisbergen, J. G. Snijders, and E. J. Baerends, Comput. Phys. Commun. (submitted).
- ⁶³ deMon-DynaRho version 2, M. E. Casida, C. Jamorski, and D. R. Salahub, University of Montreal.
- ⁶⁴ deMon-KS version 1.2, J. W. Andzelm, M. E. Casida, A. Koester, E. Proynov, A. St-Amant, D. R. Salahub, H. Duarte, N. Godbout, J. Guan, C. Jamorski, M. Leboeuf, V. Malkin, O. Malkina, F. Sim, and A. Vela, deMon Software, University of Montreal, 1995.
- ⁶⁵ T. Ziegler, A. Rauk, and E. J. Baerends, Theor. Chim. Acta **43**, 261 (1977).
- ⁶⁶ R. P. Messmer and D. R. Salahub, J. Chem. Phys. **65**, 779 (1976).
- ⁶⁷ deMon-KS version 4.0, M. E. Casida, C. Daul, A. Goursot, A. Koester, L. G. M. Pettersson, E. Proynov, A. St-Amant, and D. R. Salahub (principal authors); H. Duarte, N. Godbout, J. Guan, C. Jamorski, M. Leboeuf, V. Malkin, O. Malkina, M. Nyberg, L. Pedocchi, F. Sim, L. Triguero, and A. Vela (contributing authors); deMon Software, University of Montreal, 1997.
- ⁶⁸ S. J. A. van Gisbergen, V. P. Osinga, O. V. Gritsenko, R. van Leeuwen, J. G. Snijders, and E. J. Baerends, J. Chem. Phys. **105**, 3142 (1996).
- ⁶⁹ T. D. Bouman and A. E. Hansen, Chem. Phys. Lett. **117**, 461 (1985).
- ⁷⁰ V. Galasso, J. Mol. Struct.: THEOCHEM **168**, 161 (1988).
- ⁷¹ K. B. Wiberg, C. M. Hadad, J. B. Foresman, and W. A. Chupka, J. Phys. Chem. **96**, 10756 (1992).
- ⁷² P. R. T. Schipper, S. J. A. van Gisbergen, O. V. Gritsenko, and E. J. Baerends (unpublished).
- ⁷³ C. A. Adamo, G. E. Scuseria, and V. Barone, J. Chem. Phys. **111**, 2889 (1999).
- ⁷⁴ J. P. Perdew, K. Burke, and M. Ernzerhof, Phys. Rev. Lett. **77**, 3865 (1996); **78**, 1396 (1997).
- ⁷⁵ C. Adamo and V. Barone, J. Chem. Phys. **110**, 6158 (1999).
- ⁷⁶ M. Ernzerhof and G. E. Scuseria, J. Chem. Phys. **110**, 5029 (1999).
- ⁷⁷ M. Ernzerhof (private communication).
- ⁷⁸ O. V. Gritsenko, P. R. T. Schipper, and E. J. Baerends, Chem. Phys. Lett. **302**, 199 (1999).
- ⁷⁹ J. B. Krieger, Y. Li, and G. J. Iafrate, Phys. Lett. A **146**, 256 (1990).
- ⁸⁰ D. Sundholm, Chem. Phys. Lett. **302**, 480 (1999).
- ⁸¹ R. Bauernschmitt, R. Ahlrichs, F. H. Heinrich, and M. M. Kappes, J. Am. Chem. Soc. **120**, 5052 (1998).
- ⁸² T. N. Olney, N. M. Cann, G. Cooper, and C. E. Brion, Chem. Phys. **223**, 59 (1997).
- ⁸³ W. F. Chan, G. Cooper, R. N. S. Sodhi, and C. E. Brion, Chem. Phys. **170**, 81 (1993).
- ⁸⁴ W. F. Chan, G. Cooper, and C. E. Brion, Chem. Phys. **170**, 123 (1993).
- ⁸⁵ G. Cooper, J. E. Anderson, and C. E. Brion, Chem. Phys. **209**, 61 (1996).
- ⁸⁶ G. Cooper, T. N. Olney, and C. E. Brion, Chem. Phys. **194**, 175 (1995).
- ⁸⁷ J. Oddershede, N. E. Grüner, and G. H. F. Diercksen, Chem. Phys. **97**, 303 (1985).
- ⁸⁸ C. Filippi, C. J. Umrigar, and X. Gonze, J. Chem. Phys. **107**, 9994 (1997).
- ⁸⁹ A. Savin, C. J. Umrigar, and X. Gonze, in *Electronic Density Functional Theory: Recent Progress and New Directions*, edited by J. F. Dobson, G. Vignale, and M. P. Das (Plenum, New York, 1997).
- ⁹⁰ H. Agren, V. Carravetta, O. Vahtras, and L. G. M. Pettersson, Theor. Chem. Acc. **97**, 14 (1997).
- ⁹¹ W. J. Hunt and W. A. Goddard, Chem. Phys. Lett. **3**, 414 (1969).
- ⁹² W. J. Hunt and W. A. Goddard, Chem. Phys. Lett. **24**, 464 (1974).
- ⁹³ M. R. J. Hachey, P. J. Bruna, and F. Grein, J. Phys. Chem. **99**, 8050 (1995).
- ⁹⁴ M. E. Casida, 13th Canadian Symposium on Theoretical Chemistry, Vancouver, Canada, 2–7 August 1998 (unpublished).
- ⁹⁵ M. E. Casida and D. R. Salahub (unpublished).
- ⁹⁶ M. E. Casida, F. Gutierrez, J. Guan, F.-X. Gadea, D. Salahub, and J.-P. Daudey, J. Chem. Phys. (submitted).
- ⁹⁷ J. S. Muenter, J. Mol. Spectrosc. **55**, 490 (1975).
- ⁹⁸ D. R. Johnson, F. J. Lovas, and W. H. Kirchhoff, J. Phys. Chem. Ref. Data **1**, 1011 (1972).
- ⁹⁹ D. W. Turner, C. Baker, A. D. Baker, and C. R. Brundle, *Molecular Photoelectron Spectroscopy* (Wiley, New York, 1970).
- ¹⁰⁰ C. R. Brundle, M. B. Robin, N. A. Kuebler, and H. Basch, J. Am. Chem. Soc. **94**, 1451 (1972).
- ¹⁰¹ G. Bieri and L. Åsbrink, J. Electron Spectrosc. Relat. Phenom. **20**, 149 (1980).
- ¹⁰² J. Chem. Phys. **23**, 1997 (1955).
- ¹⁰³ U. Kaldor and S. B. Ben-Shlomo, J. Chem. Phys. **92**, 3680 (1990).
- ¹⁰⁴ E. S. Nielsen, P. Jørgensen, and J. Oddershede, J. Chem. Phys. **73**, 6238 (1980).
- ¹⁰⁵ D. J. Clouthier and D. A. Ramsay, Annu. Rev. Phys. Chem. **34**, 31 (1983).
- ¹⁰⁶ S. Taylor, D. G. Wilden, and J. Comer, Chem. Phys. **70**, 291 (1982).
- ¹⁰⁷ L. Serrano-Andrés, M. Merchán, I. Nebot-Gil, R. Lindh, and B. O. Roos, J. Chem. Phys. **98**, 3151 (1993).
- ¹⁰⁸ L. B. Harding and W. A. Goddard III, J. Am. Chem. Soc. **99**, 677 (1977).
- ¹⁰⁹ H. Nakatsuji, K. Ohta, and K. Hirao, J. Chem. Phys. **75**, 2952 (1981).
- ¹¹⁰ C. Petrongolo, R. J. Buenker, and S. D. Peyerimhoff, J. Chem. Phys. **76**, 3655 (1982).
- ¹¹¹ V. Galasso, J. Chem. Phys. **92**, 2495 (1990).
- ¹¹² K. Kirby and D. L. Cooper, J. Chem. Phys. **90**, 4895 (1989).
- ¹¹³ C. E. Bielschowsky, M. A. C. Nascimento, and E. Hollaver, J. Phys. B **23**, L787 (1990).
- ¹¹⁴ P. W. Langhoff, S. R. Langhoff, and C. T. Corcoran, J. Chem. Phys. **67**, 1722 (1977).